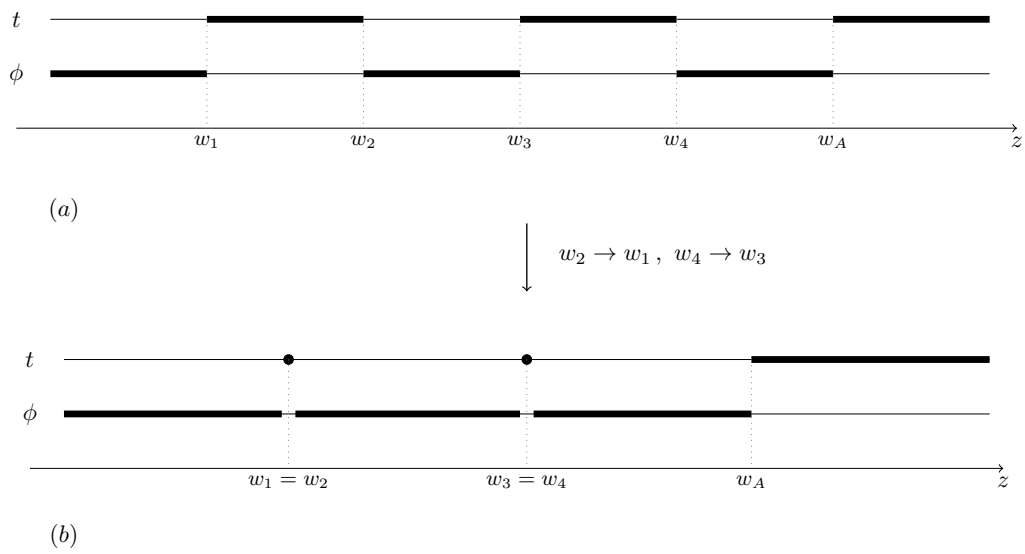

Figure 2.8: Rod diagrams for (a) the double C-metric in an external field and for (b) the Bonnor–Swaminarayan metric (2.146). We see that the limit considered in the main text $w_{2k} \to w_{2k-1}$ corresponds to shrinking the timelike rods representing the event horizons. The horizons disappear through that limit, and the resulting objects are naked singularities which are represented by points in the rod diagram.

where

$$R_k = \sqrt{\rho^2 + (z + m_k - z_k)^2}\,, \quad R_{k+1} = \sqrt{\rho^2 + (z - m_k - z_k)^2}\,, \tag{2.141}$$

we can write

$$\psi = \frac{1}{2}\log\left(\frac{R_1 + R_2 - 2m_1}{R_1 + R_2 + 2m_1}\right) + \frac{1}{2}\log\left(\frac{R_3 + R_4 - 2m_2}{R_3 + R_4 + 2m_2}\right) + \frac{1}{2}\log\mu_A\,. \tag{2.142}$$

One recognises two Schwarzschild potentials (the first two terms) and the Rindler potential (the last term). Indeed, at the level of the Weyl potential a superposition principle holds; the non-linearity is encoded in the function γ, that we do not explicitly write here.

Now we consider the limit in which the finite timelike rods of Fig. 2.6 are pinched to a point, i.e. when $w_{2k} \to w_{2k-1}$: this is equivalent to consider $m_k \to 0$ (see Fig. 2.8). We expand for small m_k to order $O\big(m_k^2\big)$, to find

$$\psi \approx -\frac{m_1}{\sqrt{\rho^2 + (z - z_1)^2}} - \frac{m_2}{\sqrt{\rho^2 + (z - z_2)^2}} + \frac{1}{2}\log\mu_A\,. \tag{2.143}$$

Again, we recognise the various terms in the last expression: the first two are Curzon–Chazy potentials and represent point-like particles, while the last term is still the Rindler one. Then it is natural to interpret the potential as the one corresponding to two accelerating particles (see Fig. 2.9).

We cast the potential in the usual Bonnor–Swaminarayan form by performing the change of coordinate $\bar{z} = 1/(2A^2) - z$, by which

$$\mu_A = \sqrt{\rho^2 + \bar{z}^2} + \bar{z}\,, \tag{2.144}$$

and then defining the new constants

$$2\alpha_1^2 = \frac{2A^2}{2A^2 z_1 - 1}\,, \quad 2\alpha_2^2 = \frac{2A^2}{2A^2 z_2 - 1}\,. \tag{2.145}$$

One finally finds

$$\psi = -\frac{m_1}{\sqrt{\rho^2 + (\bar{z} - \frac{1}{2\alpha_1^2})^2}} - \frac{m_2}{\sqrt{\rho^2 + (\bar{z} - \frac{1}{2\alpha_2^2})^2}} + \frac{1}{2}\log\big(\sqrt{\rho^2 + \bar{z}^2} + \bar{z}\big)\,, \tag{2.146}$$

which is the Bonnor–Swaminarayan potential (cf. [193] and [135]). The generalisation to N accelerating particles is easily found as

$$\psi = -\sum_{k=1}^{N} \frac{m_k}{\sqrt{\rho^2 + (\bar{z} - \frac{1}{2\alpha_k^2})^2}} + \frac{1}{2}\log\big(\sqrt{\rho^2 + \bar{z}^2} + \bar{z}\big)\,. \tag{2.147}$$

The γ function, which completes the Weyl metric (2.138), is found by quadratures.

One can check that the Bonnor–Swaminarayan metric (2.146), for generic values of the parameters, is affected by conical singularities. Such singularities can be removed only when $m_2 < 0$: in this case the axis is everywhere regular, except at the locations of the point particles. More explicitly, the regularisation is achieved for [135]

$$m_1 = -m_2 = \frac{(\alpha_1^2 - \alpha_2^2)^2}{4\alpha_1^3\alpha_2^3}\,. \tag{2.148}$$

The limit to the Bičák–Hoenselaers–Schmidt metric

The inclusion of the external gravitational field is now a simple matter: this can be done following the lines of Sec. 1.2, i.e. by means if the inverse scattering method, or via the same limiting procedure of the multi-black hole metric (2.101) above, now with the field parameters b_n turned on. In both cases, the resulting Weyl potential is

$$\psi = -\sum_{k=1}^{N} \frac{m_k}{\sqrt{\rho^2 + (\bar{z} - \frac{1}{2\alpha_k^2})^2}} + \frac{1}{2}\log\big(\sqrt{\rho^2 + \bar{z}^2} + \bar{z}\big) + \sum_{n=1}^{\infty} b_n r^n P_n\,. \tag{2.149}$$

The meaning of the terms in the potential is clear, and the function γ can be found again by quadratures. This potential specialises to the Bičák–Hoenselaers–Schmidt one [194] for $N = 1$ and $b_1 \neq 0$, $b_n = 0$ for $n > 1$, that reads

$$\psi = -\frac{m_1}{\sqrt{\rho^2 + (\bar{z} - \frac{1}{2\alpha_1^2})^2}} + \frac{1}{2}\log\big(\sqrt{\rho^2 + \bar{z}^2} + \bar{z}\big) + b_1 z\,. \tag{2.150}$$

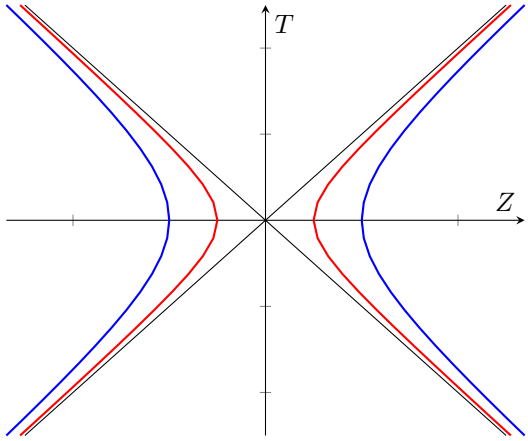

Figure 2.9: A spacetime diagram of the Bonnor–Swaminarayan metric in the boost-rotation coordinates of [195], for the section $\rho = 0$. The hyperbolae represent the world-lines of two pairs of (causally disconnected) accelerating particles.

The limiting procedure that leads to (2.149) does not affect the external field, hence it can be fine tuned again to support the particles attraction against the gravitational collapse and to remove the conical singularities.

It is worth mentioning that Bičák–Hoenselaers–Schmidt also found two accelerating particles described by internal multipole momenta [196], in analogy with the Erez–Rosen metric [141]. The multipole metric, initially obtained through a coalescing limit of the Bonnor–Swaminarayan solution, can be regularised everywhere on the z-axis (except at the two particles), thus obtaining a regular accelerating metric without the need of any external field. Relying on the discussion presented in [150], one can easily write down the most general potential for N accelerating particles with arbitrary multipole momenta and immersed in an external gravitational field:

$$\psi = -\sum_{k=1}^{N} \frac{m_k}{\sqrt{\rho^2 + (\bar{z} - \frac{1}{2\alpha_k^2})^2}} + \frac{1}{2}\log\left(\sqrt{\rho^2 + \bar{z}^2} + \bar{z}\right) + \sum_{n=1}^{\infty}\left(\frac{a_n}{r^{n+1}} + b_n r^n\right) P_n \,. \quad (2.151)$$

a_n are the internal momenta, that describe the deformations of the point-like sources. We do not delve into the details of this solution, because it is beyond our scope. However, it would be interesting to explicitly write down the function γ and to check that the conical singularities can be removed by tuning the parameters a_n and b_n.

2.5 Outlook

In this Chapter we constructed, thanks to the inverse scattering method, a large family of new solutions which generalise the Israel–Khan metric [139] and the array of accelerating black holes [180], by the introduction of an external gravitational field. We were able

to treat analytically the whole multipolar expansion of the gravitational background introducing a countable number of integration constants, characterising the gravitational multipoles of the external field, which are useful to remove all the conical singularities typical of the collinear multi-black hole configurations.

The external gravitational field can be interpreted as the centrifugal force field caused by the rotation of the two sources in a vacuum background, thanks to the equivalence principle of General Relativity, in a rotating frame located at the center of mass of a binary system. While this picture can not model a full black hole merging, it might be useful to describe a metastable stationary phase of the coalescence process, when the gravitational energy radiated by the system is still negligible, and the orbits stay almost regular.

We have computed the physical charges and verified the Smarr law for various configurations. In some particular cases, like the binary system, we also studied the thermodynamics and inspected some geometrical properties

We found that these spacetimes are relevant not only because they enrich our scarce theoretical knowledge of multi-black hole solutions or because they represent the first multi-black hole solutions which can be regularised without the need of extra fields as the electromagnetic field[18], but also because these metrics allow us to discuss some intriguing physical processes.

For example, in the case of the binary system, we were able to discuss not only the first law of thermodynamics, but also the second law: by mimicking a merging process, i.e. by comparing the initial and the final state of a merging process, we found that the entropy of the system is destined to increase. This is a non-trivial result that it is difficult to check for the usual multi-black hole metrics, because of the presence of conical defects.

Further, regularised C-metrics [19] can describe the pair creation of a couple (or possibly four in case of the double C-metric) of black holes that accelerate in opposite direction remaining causally disconnected. This process is propelled at expense of the external field, in our case the multipolar gravitational background. The significance and the novelty of our picture is given by the fact that the accelerating black hole couple can be uncharged, a feature in line with phenomenological observation.

As a by-product of our construction, we showed how to extend the vacuum Plebański–Demiański class of metrics to the rotating and accelerating multi-Kerr black holes, with or without the presence of the external gravitational field. We are also able to detect some notable known metrics as limits of our general solution describing accelerating particles with or without the external gravitational background, such as the Bonnor–Swaminarayan and the Bičák–Hoenselaers–Schmidt solutions.

[18] Actually, in the presence of Maxwell electrodynamics, Ernst showed also how to regularise the charged C-metric, thanks to an external electromagnetic field such as the Melvin universe [117]. Even though axial magnetic fields in the center of the galaxies can be of some prominence, charged black holes are not considered plausible objects because matter in the Universe is most often neutral.

[19] We notice that the single charged C-metric can be regularised without the need of an external field [197]. However, the regularisation can be achieved only in the extremal case $m = e$, which is a problematic limit for the black hole solution.

In general we have shown that, as the inverse scattering method predicts, in practice basically any diagonal seed can be used as a background for the solution generating technique. In particular, this technique reveals to be useful to embed and overlap a generic number of black hole sources, possibly providing a mechanism to regularise the conical singularities that usually afflicts these metrics. Of course, it would be interesting to explore also different backgrounds.

All these results can be extended to gravitational theories where the solution generating techniques hold, from minimally to conformally coupled scalar fields or other scalar tensor theories such as some classes of Brans–Dicke or $f(R)$ gravity.

CHAPTER 3

Black holes in an expanding bubble of nothing

We consider another example of a background which allows us to regularise a multi-black hole spacetime (again, with the aim of the inverse scattering method): the expanding Kaluza–Klein bubbles, also known as "bubbles of nothing". In the present Chapter we will also consider systems in higher spacetime dimensions, i.e. $D > 3$.

Expanding bubbles of nothing are simple but surprising solutions of gravitational theories with compact dimensions [198]. They provide channels for the non-perturbative decay of Kaluza–Klein vacua, but they are also interesting as simple time-dependent spacetimes that share many features with de Sitter cosmologies [199]. This latter view, more than the former, will be relevant in this Chapter, where we present a suggestive new way of regarding these bubbles, and investigate their relation to some black hole systems. Other aspects of the relation between black holes and bubbles of nothing have been studied in [200, 201, 202, 203, 204, 205, 206, 207, 208, 209, 210].

More specifically, we will explain that expanding bubbles of nothing are a pervasive feature of systems of black holes with multiple or non-spherical horizons[1]. To demonstrate the idea, we will show that expanding bubbles of nothing arise as a limit of static black hole binaries (in four dimensions) and of black rings (in five dimensions). These systems allow us to illustrate a general phenomenon using explicit exact solutions of vacuum gravity. We expect that versions of all the constructions are possible in six or more dimensions, but then the solutions must be obtained numerically. Other lesser-known kinds of bubbles, in five or more dimensions, arise from different black hole binaries and will be briefly examined. Towards the end of the Chapter we will discuss more general configurations using topological arguments, and argue that expanding bubbles are also present in systems such as the Schwarzschild–de Sitter and Nariai solutions.

We will also study how the expansion in bubble spacetimes acts on gravitationally interacting systems, in a manner similar to inflation in de Sitter. We will show that bubbles in four and five dimensions admit within them black hole binaries and black rings in static (although unstable) equilibrium, their attraction being balanced against the expansion of the background spacetime. The same mechanism is expected to work in more general situations for which exact solutions are not available. The present Chapter is based on the paper [211].

[1] The precise notion of the topology that is required will become clearer below.

3.1 Black holes, black rings and Kaluza–Klein bubbles

3.1.1 Expanding bubbles of nothing from black hole binaries and black rings

The solution for an expanding bubble of nothing was originally presented in [198] in the form

$$ds^2 = r^2(-dT^2 + \cosh^2 T d\Omega_n) + \frac{dr^2}{1-\frac{r_0^n}{r^n}} + \left(1-\frac{r_0^n}{r^n}\right) r_0^2 d\phi^2 \,, \tag{3.1}$$

where $d\Omega_n$ is the standard n-dimensional sphere element. This is obtained from the Schwarzschild–Tangherlini solution in $n+3$ dimensions by rotating to imaginary values the time coordinate and one polar angle. However, the relation between black holes and bubbles that we will discuss is of a different kind and does not involve any such rotation. Since the coordinate ϕ must be periodically identified, $\phi \sim \phi + 4\pi/n$, the solution has Kaluza–Klein asymptotics, but the latter fact will also be of minor relevance for our discussion.

To understand the geometry, observe that the time-symmetric section at $T = 0$ is the product of a "cigar" along the (r, ϕ) directions, and spheres S^n of radius r. These spheres cannot be shrunk to zero size since they reach a minimum radius at $r = r_0$[2]. The minimal sphere constitutes the bubble of nothing, and when it evolves for $T > 0$, it expands in a de Sitter-like fashion.

The coordinates in (3.1) cover the spacetime globally, but we can also write it using static-patch coordinates[3], where

$$ds^2 = r^2\left[-(1-\xi^2)dt^2 + \frac{d\xi^2}{1-\xi^2} + \xi^2 d\Omega_{n-1}\right] + \frac{dr^2}{1-\frac{r_0^n}{r^n}} + \left(1-\frac{r_0^n}{r^n}\right) r_0^2 d\phi^2 \,. \tag{3.2}$$

We could set $\xi = \cos\theta$ to relate it more manifestly to the Schwarzschild–Tangherlini solution with imaginary t and ϕ, but the form above makes clearer the existence of a de Sitter-like horizon at $\xi^2 = 1$. In the full spacetime, this is an infinite acceleration horizon that extends from the bubble at $r = r_0$ to infinity. Observers who sit on the bubble midpoint between the horizons, that is, near $r = r_0$ and around $\xi = 0$, find themselves partly surrounded (but not enclosed) by a horizon with topology $S^{n-1} \times \mathbb{R}^2$. Like in de Sitter, these observers do not have access to the entire S^n bubble. They only see the half of it that remains static, while the portion of the bubble beyond the horizon expands exponentially.

Let us examine the case $n = 1$ of a four-dimensional expanding bubble. This is seldom considered when studying Kaluza-Klein spacetimes, but we will give it a new twist. The sphere S^{n-1} now consists of the two endpoints of the interval $-1 \leq \xi \leq 1$, so the observer in the bubble lies between two approximately planar (for $r \approx r_0$) acceleration horizons. Such Rindler-type horizons are known to describe the geometry near a black hole, and we will find that this interpretation is also apt for the bubble

[2]The manifold can not be extended beyond $r = r_0$, thus such a point does not represent an actual singularity of the spacetime. Moreover, the Kretschmann scalar is well behaved at $r = r_0$.

[3]The change is $t = \operatorname{arctanh}(\tanh T/\cos\chi)$, $\xi = \cosh T \sin\chi$, where χ is a polar angle of S^n.

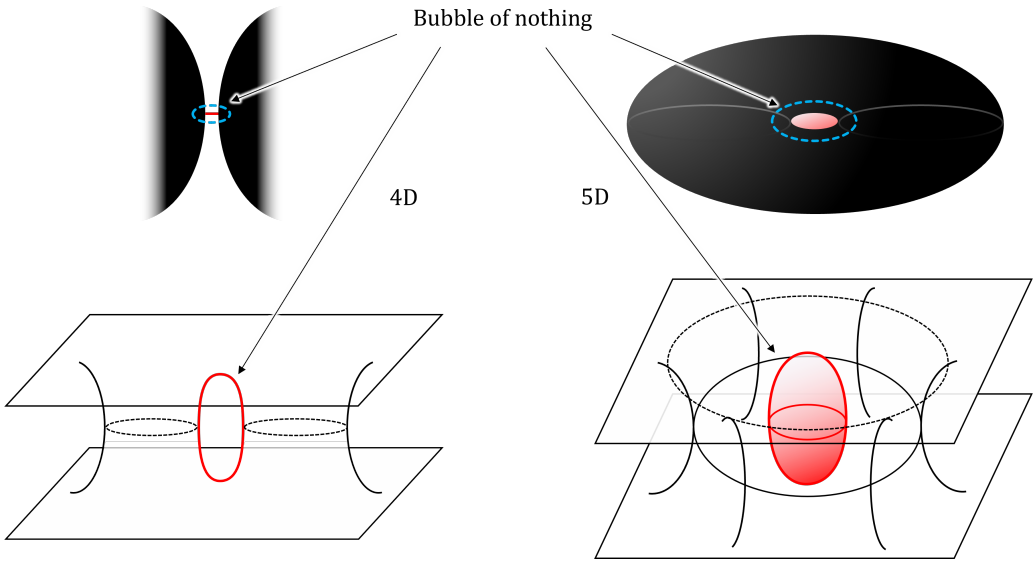

Figure 3.1: Bubbles of nothing as limits of black hole systems. The top pictures are illustrative cartoons, and the bottom ones show time-symmetric spatial sections of the maximally extended solutions. Left top: the 4D bubble of nothing arises as the geometry in between two black holes, in the limit when their size is very large. The horizons of the black holes correspond to acceleration horizons of the bubble. Left bottom: the bubble is a minimal circle (in red) linking the Einstein–Rosen throats of the two black holes. This circle encloses "nothing", and its expansion occurs as the throats stretch in the black hole interiors. The angle ϕ around the rotation axis is suppressed in these figures. Right top: the 5D bubble is similarly recovered from the central region of a very fat black ring. Right bottom: the bubble is a sphere (in red) that wraps the portion of the Einstein–Rosen bridge in the inner "hole" of the ring. In the bottom figure, the ring's S^2 is not represented. In the solutions we discuss, the black hole binary and the black ring are kept static by semi-infinite cosmic strings and cosmic membranes (not shown), respectively, which pull them outwards, but other means of maintaining them in equilibrium are possible.

geometries (3.2). That is, we will show that the four-dimensional bubble appears as the geometry in between two black holes, when they are separated by a distance much smaller than their radius (see Fig. 3.1).

One may wonder in what sense can a black hole binary contain an expanding bubble. The answer is much the same as for the static-patch metric (3.2). When $n = 1$, the bubble is a circle that links the Einstein–Rosen bridges of the black hole pair, i.e. a minimal cycle that encloses nothing (Fig. 3.1, bottom left)[4]. The static observer in between the two black holes is limited by the horizons to only have access to a portion of this circle, namely, the segment of the axis between the two horizons. The rest of the circle lies beyond the horizons. Initially, at $T = 0$, this other half-circle is another segment between the two Einstein–Rosen throats. As T evolves, these throats stretch, so the portions of the circle inside the black holes expand in time. The expansion of the bubble is then the familiar stretching that occurs in the interior of the black hole[5]. The compactification of the ϕ direction is a consequence of focusing on a small region around the symmetry axis, so the radius of the ϕ circles can only reach a finite maximum.

Exact solutions for a static configuration of a pair of black holes, kept apart by semi-infinite cosmic strings that pull on them, have been known for long [138, 139]. We will use them to explicitly exhibit the limit where they reduce to (3.2). We emphasize that there is no Wick-rotation involved in this connection: the time and angular coordinates retain their physical meaning throughout the limit.

The five-dimensional bubble, described originally in [198], also admits a similar interpretation. Now the acceleration horizon, with topology $S^1 \times \mathbb{R}^2$, is connected. We will find that (3.2) with $n = 2$ arises as the limit of a black ring, with horizon topology $S^1 \times S^2$, when the size of the S^2 is much larger than the inner rim of the ring circle. The static coordinates only cover the hemisphere of the S^2 bubble that consists of the disk of the inner "hole" of the ring. In global coordinates, the S^2 is a minimal sphere that wraps the Einstein–Rosen bridge in the inner hole of the ring. In this case, we will use the solution, first found in [200], for a static black ring held in place by an infinite cosmic membrane attached to the outer rim of the ring. We expect that this construction generalizes to all $n \geq 3$, but the required solutions, with horizons of topology $S^{n-1} \times S^2$, are only known numerically [213, 214].

We will also briefly discuss how a certain type of five-dimensional black hole binary, in the limit of small separation, gives rise to a five-dimensional expanding bubble of a different kind than the $n = 2$ bubble above: the minimal cycle is not a single sphere S^2, but two S^2 that lie on orthogonal spaces and which touch each other at both North and South poles. They compactify the spacetime on a two-torus (instead of a circle). A more general discussion of the topology of other configurations will be presented in the concluding Section.

[4]Strictly speaking, the cycle Ω_1 in (3.1) need not be a compact S^1 (it might be a non-compact $\mathbb{R}$, that gives rise to a different topology), but we will take it to be so. In the binary, we are identifying asymptotic regions to yield the smallest maximal analytic extension.

[5]The same effect is responsible for the growth of holographic volume complexity[212].

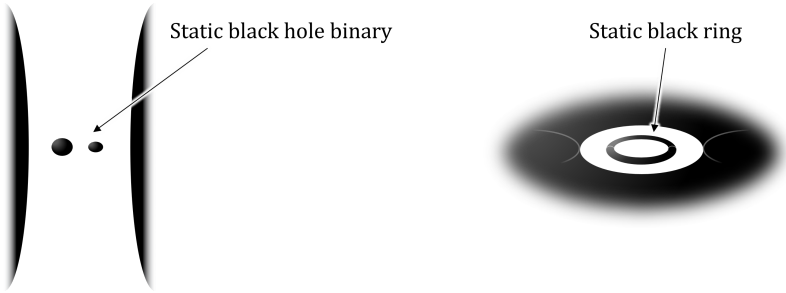

Figure 3.2: Static black hole binaries and black rings obtained by placing them inside expanding bubbles of nothing, which surround them with acceleration horizons. The binary need not be symmetrical. These configurations can be regarded as limits of double nested static binaries (four black holes along a line), and of two coaxial black rings.

Let us mention that the specific mechanism that keeps the black hole pair, or the black ring, in static equilibrium is not an essential aspect of the construction. Cosmic strings and membranes, in the form of conical deficits along the outer symmetry axes of the systems, are easy to work with, but the two black holes could also carry electric charges of opposite sign (a dihole [215, 176]) and be held in equilibrium by an external electric field, namely, a fluxbrane. A similar construction is also possible for dipole black rings [216]. As long as the black holes are not extremal, they will have bifurcation surfaces and there will be expanding bubbles, with the effects of the electric field becoming negligible in the region between the horizons, since the external fluxbrane polarizes the system so as to cancel the opposite fluxbrane-like field between the charged black holes [217]. Other equilibration methods are possible, but their differences only show up far from the gap between the horizons. In the limit to the bubble solution, the distinctions between these geometries disappear.

Indeed, the explanation we have given should make clear, and we will elaborate further on this in the concluding Section, that, as long as the black holes in a binary have bifurcate horizons, expanding bubbles are also present in them even if the horizons are not static but dynamically merge and collapse. But in these cases the expansion of the bubble only lasts a finite time.

3.1.2 Black hole binaries and black rings inside expanding bubbles

The previous remarks bring us to the other main subject of this Chapter, namely, the static equilibrium configurations of black hole binaries and black rings.

A possibility for balancing the attraction in the binary is the expansion of spacetime. Indeed, one expects that such binaries in (unstable) equilibrium exist in the de Sitter universe, but the solutions can only be constructed approximately for very small black holes, or numerically [218]. Nevertheless, the expansion in a bubble should achieve the same effect. To prove this, we will construct exact solutions where an expanding bubble hosts a black hole binary (see Fig. 3.2 left) (possibly with different masses) in

static equilibrium. The interpretation of the expanding bubbles given above provides another explanation for why this is possible: we can introduce a binary of two small black holes in the gap between two very large black holes, and then tune the distances between them so that the attraction in the small binary is balanced by the pull of the larger black holes.

The analogues of these configurations involving black rings in five dimensions can also be readily constructed (see Fig. 3.2 right). We will present a solution for a static black ring inside a five-dimensional bubble of nothing, and show that it can be recovered as the limit of a concentric, static double black ring system.

All these metrics can be given in exact closed form since they are Weyl solutions, which admit a systematic construction with an arbitrary number of collinear black holes, or concentric black rings [219, 138, 139, 200]. The configurations are characterized by their rod structure [200, 137], which specifies the sources along the different symmetry axes. This structure makes transparent the features of all the constructions discussed above and their limits. Indeed, the connections between the black hole binary and the static black ring, and the corresponding expanding bubbles in four and five dimensions, have been apparent at least since the analysis in [200]. Nevertheless, to our knowledge, this connection does not appear to be widely known, and it has not been examined in detail in the literature.

3.2 Bubbles as limits of black hole binaries and black rings

We will now show explicitly how the metrics for the bubbles of nothing in 5D and 4D are recovered as limits of static black ring and binary black hole solutions in the manner illustrated in Fig. 3.1.

3.2.1 From black ring to bubble

The simplest instance is the relationship between the five-dimensional bubble of nothing of [198] and the static black ring of [200]. The metric of the latter is

$$\begin{aligned} ds^2 = &-\frac{F(x)}{F(y)}d\tilde{t}^2 + \frac{R^2}{(x-y)^2}\left[F(x)\left((y^2-1)d\tilde{\psi}^2 + \frac{F(y)}{y^2-1}dy^2\right)\right. \\ &\left. + F(y)^2\left(\frac{dx^2}{1-x^2} + \frac{1-x^2}{F(x)}d\tilde{\phi}^2\right)\right], \end{aligned} \tag{3.3}$$

with

$$F(\xi) = 1 - \mu\xi\,. \tag{3.4}$$

Readers unfamiliar with these (x, y) coordinates are referred to [200] and [98] for a detailed explanation. Roughly, $x \in [-1, 1]$ is the cosine of the polar angle of the ring's S^2, and $-1/y \in (0, -1/x)$ is a radial coordinate away from these spheres. The coordinates $\tilde{\psi}$ and $\tilde{\phi}$ are, respectively, the angle of the S^1 and the azimuthal angle of the S^2 of the black ring. The parameter R sets the scale for the size of the black ring, and varying

$\mu \in [0,1)$ changes its shape from thin to fat. The horizon lies at $y=-\infty$, and the absence of conical singularities along the $\tilde{\psi}$ rotation axis at $y=-1$, and in the inner disk of the ring at $x=1$, is obtained when we identify

$$\tilde{\psi} \sim \tilde{\psi} + 2\pi\sqrt{1+\mu}\,, \qquad \tilde{\phi} \sim \tilde{\phi} + 2\pi\sqrt{1-\mu}\,. \tag{3.5}$$

In order to make the ring very big and fat, and to blow up the inner disk region, we will take $\mu \to 1$ and $R \to \infty$ while zooming in onto $x \approx 1$. For this purpose, we change

$$x = 1 - \frac{r^2 - r_0^2}{2R^2}\,, \qquad \mu = 1 - \frac{r_0^2}{2R^2}\,, \tag{3.6}$$

where r and r_0 are a new coordinate and a constant parameter that remain finite as $R \to \infty$. In addition we introduce a coordinate ξ via

$$y = -\frac{1+\xi^2}{1-\xi^2}\,, \tag{3.7}$$

and rescale the Killing coordinates to have canonical normalization,

$$\tilde{t} = 2Rt\,, \qquad \tilde{\psi} = \sqrt{2}\psi\,, \qquad \tilde{\phi} = \frac{r_0}{\sqrt{2}R}\phi\,. \tag{3.8}$$

Then, in the limit $R \to \infty$, the metric (3.3) becomes

$$ds^2 \to r^2\left(-(1-\xi^2)dt^2 + \frac{d\xi^2}{1-\xi^2} + \xi^2 d\psi^2\right) + \frac{dr^2}{1-\frac{r_0^2}{r^2}} + \left(1-\frac{r_0^2}{r^2}\right)r_0^2 d\phi^2\,, \tag{3.9}$$

which is indeed the same as the metric (3.2) of the bubble of nothing for $n=2$.

Observe that the ϕ circles in (3.9) cannot reach arbitrarily large sizes but become a compact direction at infinity. This is a consequence of focusing on the region close to the disk at $x=1$, which limits the growth of these circles.

One might wonder whether rotating black rings, with the rotation adjusted to balance the tension and gravitational self-attraction, have a limit to the bubble of nothing. The answer is no: in the limit where the rotating ring becomes very fat, it approaches a singular, horizonless solution instead of the non-singular geometry (3.9).

3.2.2 Weyl metrics and rod structures

All other solutions in this chapter will be presented as vacuum Weyl metrics, using cylindrical coordinates

$$ds^2 = f(\rho,z)\big(d\rho^2 + dz^2\big) + g_{ab}(\rho,z)dx^a dx^b\,. \tag{3.10}$$

We have already presented such a metric in Sec. 1.2, nevertheless we will provide a broader overview in the context of higher-dimensional spacetimes. For more complete expositions, we refer to [133, 200, 99, 137]. The main feature of (3.10) is the presence of $D-2$ Killing coordinates x^a: in four dimensions they are (t,ϕ), and in five dimensions they include an additional angle, (t,ϕ,ψ).

For all the solutions presented here, the metric $g_{ab}(\rho, z)$ along the Killing directions will be diagonal. Static and axisymmetric solutions can then be systematically constructed by specifying a set of rod-like sources along the z-axis for the three-dimensional Newtonian potentials associated to the metric functions g_{ab}; they are not physical rods, but coordinate singularities in the axis $\rho = 0$ of the Weyl metrics. Their importance derives from the fact that, given the rod distribution, the form of $g_{ab}(\rho, z)$ directly follows from a simple algebraic construction. Subsequently, $f(\rho, z)$ can be obtained by a line integral in the case of diagonal metrics, and more generally by the inverse scattering method [133]. The rods (with linear density $1/2$) are specified along each direction x^a, in such a way that at every value of z there is a rod along one and only one of the directions.

The rod structure provides an easy diagrammatic way to interpret static (or more generally stationary) axisymmetric solutions. On a rod along a direction x^a, the corresponding Killing vector has a fixed point set. When we have an angular Killing vector, such as ∂_ϕ or ∂_ψ, then the corresponding circles shrink to zero size at the rod, and the periodicity of the angle must be appropriately chosen in order to avoid conical singularities. The regularity condition on $x^a \sim x^a + \Delta x^a$ at any given rod is

$$\Delta x^a = 2\pi \lim_{\rho\to 0} \rho \sqrt{\frac{f}{g_{aa}}} \,. \tag{3.11}$$

When the Killing vector is timelike ∂_t, the rod represents a horizon, and through Euclidean continuation $t \to i\tau$, Eq. (3.11) gives its associated temperature $T = \Delta\tau^{-1}$. If the rod is finite, it defines an event horizon, while infinite rods are generically associated to accelerating horizons, such as Rindler ones.

The topology of the solutions can also be inferred from the rod structure. If there is a rod along a direction x^a, the other directions x^b are fibered along the corresponding portion of the axis. At a point where rods along x^a and x^b meet, the two fibers shrink to zero. As a result, the solutions have a "bubbling" structure.

To illustrate these features we will describe the simplest examples that are relevant to us here.

Four-dimensional solutions

The Schwarzschild black hole rod structure is given by a finite timelike rod and two semi-infinite spacelike rods (see Fig. 3.3(a)). The four-dimensional bubble of nothing is the double Wick-rotated version of the Schwarzschild metric, thus its rod structure is consistently given by exchanging the t and ϕ rods of the previous solution (see Fig. 3.3(b)). We see from their respective timelike rods that in the Schwarzschild solution the horizon is finite, while the bubble of nothing possesses two infinite acceleration horizons.

The corresponding metrics are given by

$$g_{ab}^{\text{Schwarz}} dx^a dx^b = -\frac{\mu_1}{\mu_2} dt^2 + \rho^2 \frac{\mu_2}{\mu_1} d\phi^2 \,, \tag{3.12}$$

$$g_{ab}^{\text{bubble}} dx^a dx^b = -\rho^2 \frac{\mu_2}{\mu_1} dt^2 + \frac{\mu_1}{\mu_2} d\phi^2 \,, \tag{3.13}$$

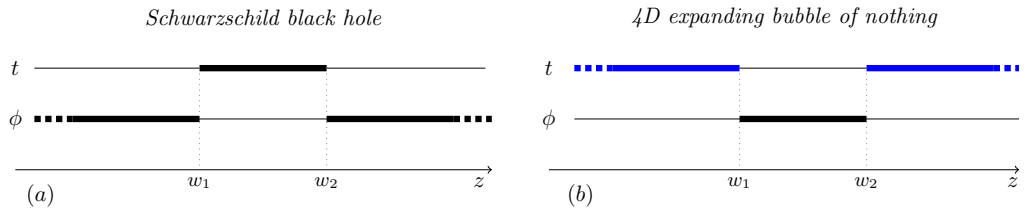

Figure 3.3: (a) rod diagram for the Schwarzschild black hole. The finite timelike rod defines the black hole horizon (a sphere S^2, from the fibration of the ϕ parallel circles over the segment $w_1 < z < w_2$). Exchanging $t \to \phi$ gives (b): rod diagram of the expanding bubble of nothing. The semi-infinite timelike rods represent the bubble acceleration horizons (two of them, each with topology $\mathbb{R}^2$). Here and in the following figures, acceleration horizons are pictured in blue.

and, in both cases,

$$f = C_f \frac{4\mu_1\mu_2^3}{\mu_{12}W_{11}W_{22}}\,. \tag{3.14}$$

Here, and in the following, we introduce

$$\mu_i = w_i - z + \sqrt{\rho^2 + (z-w_i)^2}\,, \qquad \mu_{ij} = (\mu_i - \mu_j)^2\,, \qquad W_{ij} = \rho^2 + \mu_i\mu_j\,. \tag{3.15}$$

The parameters w_i, chosen in increasing order, specify the rod endpoints, and they define the physical properties of the metric: the position of the horizons, the size and mass of the black holes, and the rotation axes. The parameter C_f is an arbitrary gauge constant. It corresponds to a rescaling of ρ and z, and it can be chosen, without loss of generality, to fix the normalization of one of the Killing directions, for instance, setting the periodicity of one of the angles to any prescribed value, such as canonical periodicity 2π.

It is now straightforward to verify that taking

$$w_1 = z_0 - \frac{r_0}{2}\,, \qquad w_2 = z_0 + \frac{r_0}{2}\,, \qquad C_f = r_0^2\,, \tag{3.16}$$

and defining

$$\rho = \sqrt{r(r-r_0)}\sin\theta\,, \qquad z = z_0 + \left(r - \frac{r_0}{2}\right)\cos\theta\,, \tag{3.17}$$

in (3.12) and (3.14), we recover

$$g_{ab}^{\text{Schwarz}}dx^a dx^b = -\left(1 - \frac{r_0}{r}\right)dt^2 + r^2\sin^2\theta d\phi^2\,, \tag{3.18}$$

$$g_{ab}^{\text{bubble}}dx^a dx^b = -r^2\sin^2\theta dt^2 + \left(1 - \frac{r_0}{r}\right)d\phi^2\,, \tag{3.19}$$

and

$$f(\rho,z)\left(d\rho^2 + dz^2\right) = \frac{dr^2}{1-\frac{r_0}{r}} + r^2 d\theta^2\,, \tag{3.20}$$

which are the conventional forms of the Schwarzschild and bubble solutions (up to possible constant rescalings of the Killing coordinates t and ϕ). They are obviously equiva-

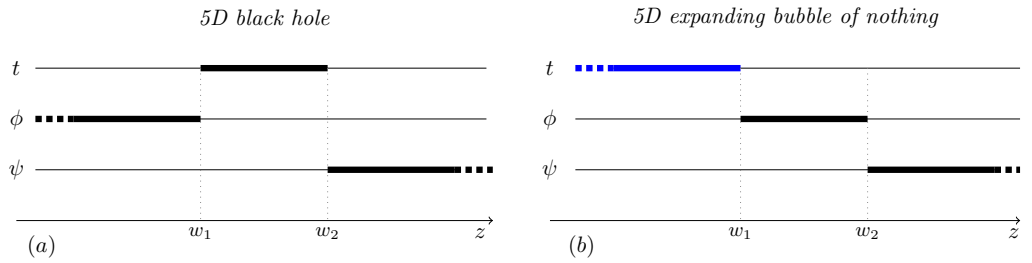

Figure 3.4: (a): rod diagram for the 5D Tangherlini black hole. The finite timelike rod defines the black hole horizon (a sphere S^3, fibering ϕ and ψ circles over $w_1 < z < w_2$). Exchanging $t \leftrightarrow \phi$ gives (b): rod diagram of the five-dimensional expanding bubble of nothing. The timelike semi-infinite rod represents the bubble acceleration horizon (which is connected, with topology $S^1 \times \mathbb{R}^2$: the ψ circles are trivially fibered over $-\infty < z < w_1$).

lent under $t \leftrightarrow \phi$. The form of the bubble of nothing in (3.2) is recovered by rescaling ϕ by r_0[6], and setting $\cos\theta = \xi$.

Finally, observe that if in either of the solutions we send one of the rod endpoints, w_1 or w_2, to infinity while keeping the other fixed, then we recover the geometry of Rindler space, with an infinite acceleration horizon. The Minkowski spacetime can be obtained when both the poles are simultaneously pushed infinitely far away in opposite directions, i.e. $w_1 \to -\infty$ and $w_2 \to \infty$.

Five-dimensional solutions

The previous analysis has a straightforward counterpart in five dimensions. The rod structures of the Schwarzschild–Tangherlini black hole and the five-dimensional expanding bubble are given in Fig. 3.4, which makes evident that they are related by a double-Wick rotation that effectively exchanges t and ϕ.

These rod structures dictate that

$$g_{ab}^{\text{Tang}} dx^a dx^b = -\frac{\mu_1}{\mu_2} dt^2 + \frac{\rho^2}{\mu_1} d\phi^2 + \mu_2 d\psi^2 \,, \tag{3.21}$$

$$g_{ab}^{\text{5D-bubble}} dx^a dx^b = -\frac{\rho^2}{\mu_1} dt^2 + \frac{\mu_1}{\mu_2} d\phi^2 + \mu_2 d\psi^2 \,, \tag{3.22}$$

while $f(\rho, z)$ is again identical for both spacetimes

$$f = C_f \, \frac{\mu_2 W_{12}}{W_{11} W_{22}} \,. \tag{3.23}$$

To express the Tangherlini black hole in spherical coordinates

$$ds^2 = -\left(1 - \frac{r_0^2}{r^2}\right) dt^2 + \frac{dr^2}{1 - \frac{r_0^2}{r^2}} + r^2 d\theta^2 + r^2 \sin^2\theta d\phi^2 + r^2 \cos^2\theta d\psi^2 \,, \tag{3.24}$$

[6]We could have achieved this by adequately choosing C_f, but, in general, we will not take ϕ to be canonically normalized with $\phi \sim \phi + 2\pi$, but rather its periodicity will be suitably adjusted.

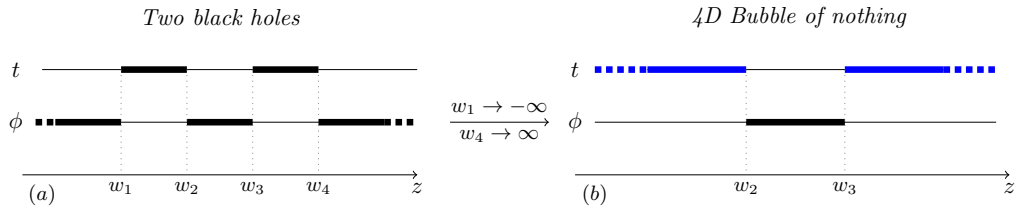

Figure 3.5: (a) Rod diagram for the Bach–Weyl static binary black hole configuration [138]. The thick timelike rods represent the two black hole horizons. By sending the rod endpoints $w_1 \to -\infty$, $w_4 \to \infty$, with w_2 and w_3 fixed, we recover the same diagram as in the bubble of nothing Fig. 3.3(b). This limit makes the two black holes infinitely large, while keeping the separation between them finite, as is illustrated in panel (b).

we choose

$$w_1 = z_0 - \frac{r_0^2}{4}\,, \qquad w_2 = z_0 + \frac{r_0^2}{4}\,, \qquad C_f = 1\,, \tag{3.25}$$

and change

$$\rho = \frac{r}{2}\sqrt{r^2 - r_0^2}\,\sin 2\theta\,, \qquad z = z_0 + \frac{1}{4}\left(2r^2 - r_0^2\right)\cos 2\theta\,. \tag{3.26}$$

Similarly, the five-dimensional expanding bubble in spherical coordinates takes the form

$$ds^2 = -r^2\cos^2\theta dt^2 + \frac{dr^2}{1-\frac{r_0^2}{r^2}} + r^2 d\theta^2 + \left(1 - \frac{r_0^2}{r^2}\right)d\phi^2 + r^2\sin^2\theta d\psi^2\,. \tag{3.27}$$

When we rescale ϕ by r_0 and set $\sin\theta = \xi$ we recover (3.9).

3.2.3 From binary black hole to bubble

Now let us consider the Bach–Weyl solution, with

$$g_{ab}dx^a dx^b = -\frac{\mu_1\mu_3}{\mu_2\mu_4}d\tilde{t}^2 + \rho^2\frac{\mu_2\mu_4}{\mu_1\mu_3}d\tilde{\phi}^2\,, \quad f = \frac{16\tilde{C}_f\,\mu_1^3\mu_2^5\mu_3^3\mu_4^5}{\mu_{12}\mu_{14}\mu_{23}\mu_{34}W_{13}^2W_{24}^2W_{11}W_{22}W_{33}W_{44}}\,, \tag{3.28}$$

which describes two Schwarzschild black holes aligned along the z-axis, and whose rod diagram is pictured in Fig. 3.5(a). By appropriately choosing $\tilde{C}_f$ to be

$$\tilde{C}_f = 16(w_1-w_2)^2(w_1-w_3)^2(w_2-w_4)^2(w_3-w_4)^2\,, \tag{3.29}$$

we make the segment $w_2 < z < w_3$ of the axis in between the black holes regular, while keeping the standard periodicity of the azimuthal angle $\Delta\phi = 2\pi$. On the other hand, along the semi-infinite axes from the black holes towards $z \to \pm\infty$ there are conical deficits. These can be regarded as cosmic strings that keep the black holes apart.

The rod diagram makes manifest how this solution is connected to other black hole/bubble configurations, either via double-Wick rotations that exchange the t and ϕ rods[7], or by

[7]The Bach–Weyl solution is the double-Wick rotation of the single black hole in the bubble [201]

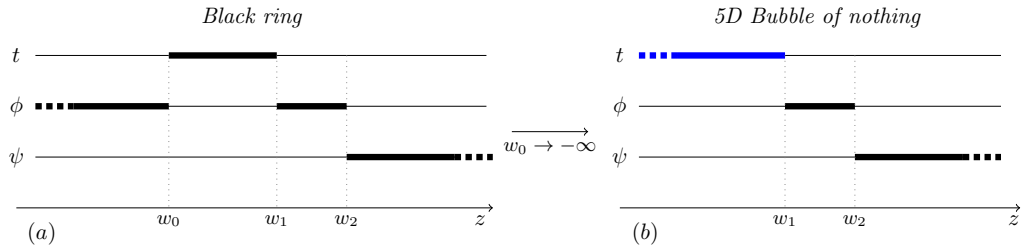

Figure 3.6: (a) Rod diagram for the static black ring. The thick timelike rod represents the black ring horizon, with topology $S^1 \times S^2$. (b) By sending the rod endpoint $w_0 \to -\infty$, with w_1 and w_2 fixed, we recover the bubble of nothing in Fig. 3.4(b). This limit makes the black ring very fat, while keeping its hole finite, as was illustrated in Fig. 3.1.

taking limits where rod endpoints merge or are sent to infinity. For our purposes here, we observe that by simply sending the rod endpoints $w_1 \to -\infty$ and $w_4 \to \infty$, with w_2 and w_3 fixed, we recover the rod diagram of the 4D bubble of nothing, Fig. 3.3(b). When we do so, we make the two black holes infinitely large, while maintaining fixed the separation between them. This is precisely the type of limit that we discussed in the introduction (see Fig. 3.1). The cosmic strings collapse the space along the outer axes creating a conical deficit angle of 2π, but this is not a problem since this part of the geometry is pushed away to infinity.

To see that the limit works correctly, not only with the rods but also in the entire metric, we conveniently place the bubble poles symmetrically at $w_1 = -z_b$ and $w_4 = z_b$. Then, we rescale

$$\tilde{t} = (2z_b)t\,, \qquad \tilde{\phi} = \frac{\phi}{2z_b}\,, \tag{3.30}$$

so that the metric (3.28) remains finite when we send $z_b \to \infty$. One can readily verify that, after rescaling $\tilde{C}_f = C_f/4$ to take into account that in (3.12) ϕ has periodicity 4π, the bubble of nothing in the form of (3.12) and (3.14) is recovered.

We have then proven that the gravitational field of the expanding bubble is indeed the same as that between two very large black holes.

3.2.4 From black ring to bubble, Weyl style

It is now easy to see how the rod diagrams also make transparent the limit from the static black ring to the expanding bubble of nothing, which we discussed using other coordinates in Sec. 3.2.1.

Fig. 3.6(a) shows the rod diagram for the static black ring. The Weyl form of the metric that follows from the diagram is

$$g_{ab}dx^a dx^b = -\frac{\mu_0}{\mu_1}d\tilde{t}^2 + \rho^2\frac{\mu_1}{\mu_0\mu_2}d\tilde{\phi}^2 + \mu_2 d\psi^2\,, \qquad f = C_f\frac{\mu_2 W_{01}^2 W_{12}}{W_{02}W_{00}W_{11}W_{22}}\,. \tag{3.31}$$

The horizon of the black ring, with topology $S^1 \times S^2$, lies at $w_0 < z < w_1$, while the "hole" of the ring is in the region $w_1 < z < w_2$. If we send $w_0 \to -\infty$ keeping all other

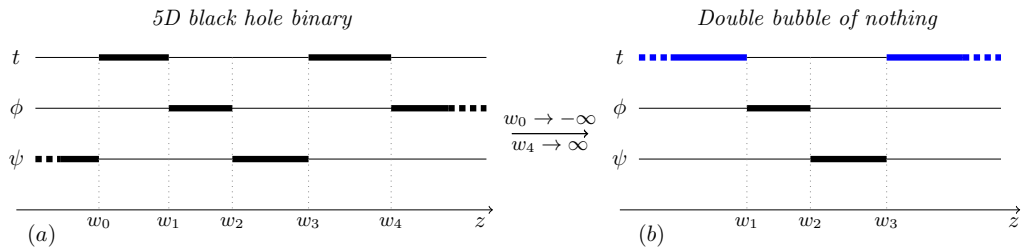

Figure 3.7: (a) Rod diagram for the five-dimensional black hole binary of [220]. (b) Limit to the expanding bubble of nothing of Sec. 4.7 in [200], which is asymptotic to a space compactified on a two-torus. The space in between the horizons, $w_1 < z < w_3$, consists of two topological disks D_2, orthogonal to each other and touching at their origins (at $z = w_2$). In the maximal analytic extension, these become two orthogonal S^2 that touch at their poles.

rod endpoints fixed (hence making the ring very fat while its hole remains finite) we recover the same diagram as for the expanding bubble of nothing in Fig. 3.4(b). In the metric, this requires a suitable rescaling of t and ϕ, similarly to what happens in the 4D case. The required rescalings are

$$\tilde{t} = \sqrt{2|w_0|}t\,, \qquad \tilde{\phi} = \frac{\phi}{\sqrt{2|w_0|}}\,. \tag{3.32}$$

3.2.5 Five-dimensional black hole binaries and bubbles

We shall briefly mention how a limit can be taken in a five-dimensional black hole binary that is asymptotically flat (save for possible conical defect membranes) to yield a different kind of five-dimensional expanding bubble.

The Weyl formalism allows to combine two five-dimensional Tangherlini black holes with the rod structure in Fig. 3.7(a). This system was studied in [220]. Since the two black holes lie along different axes, they cannot be regarded as collinear. Nevertheless, the solution is asymptotically flat, as follows from the presence of one semi-infinite rod along ϕ and another along ψ. Now take, as in the previous examples, the limit where the two black holes become infinitely large, making their timelike rods semi-infinite. The result is the system in Fig. 3.7(b).

This geometry was analyzed in [200], where one can find the explicit solution (see Sec. 4.7 there). Here we shall only describe its main properties. Conical singularities can be avoided along all the axes, and the solution is identified as an expanding bubble of nothing. In contrast to the simpler five-dimensional bubble of (3.9) (and (3.22)), where the minimal cycle (the bubble) is a sphere S^2, in this case it is made of two orthogonal S^2, i.e., the meridian lines of one sphere are orthogonal to the meridian lines of the other, and the parallel lines of one lie along ϕ and of the other along ψ. The two spheres touch each other at both their north and south poles. Furthermore, the single bubble in (3.9) asymptotically has one compact circle, while the double bubble in Fig. 3.7(b)

has two, and therefore represents a Kaluza–Klein compactification from five to three dimensions. Each of the two S^2 is responsible for the compactification of one of the two circle directions. The solution also differs from the four-dimensional bubble (3.19), in that the two acceleration horizons here are not symmetric: the ϕ and ψ circles close off at one or the other horizon, and their accelerations can be different. Indeed, the two S^2 can have different sizes.

The two five-dimensional black holes can also be combined in a different fashion with Kaluza–Klein asymptotics [200, 202]. The configuration has a limit to a "bubble string", i.e., the direct product of the 4D expanding bubble and a circle. Ref. [200] showed that the Weyl formalism allows to generalize all of these solutions to other expanding bubbles in higher dimensions, which compactify spacetime down to three or four dimensions.

Finally, we could envisage starting from a collinear pair of 5D black holes which lie along a line that is a fixed point of $SO(3)$ rotations (and not $SO(2)$, as above). In this case, the limit of small separation would result, like in 4D, in a topologically circular S^1 bubble. However, these configurations (and their higher-dimensional counterparts) do not fall within the Weyl class, and they are not known in exact form.

3.3 Static black hole binaries and black rings in expanding bubbles

In this section, we will explore some configurations in 4D and 5D that can be regularised by the presence of an expanding bubble of nothing. First, we will consider a 4D static black hole binary system (a subcase of the Israel–Khan solution [139]). As is well known, the Bach–Weyl binary in (3.28) necessarily contains conical singularities on the axis $\rho = 0$, either in the segment in between the two black holes, or (as we chose above) in the semi-axes towards infinity: these are, respectively, struts or strings that balance the attraction between the black holes. We will prove how, by placing the binary within the bubble, we can remove all these singularities and thus obtain a completely regular system on and outside the event horizons.

An analogous construction is possible for the 5D static black ring. In the manner we presented this solution in Secs. 3.2.1 and 3.2.4, the geometry is singular because the tension and self-attraction of the ring, which would drive it to collapse, need to be balanced by a conical-defect membrane. Again, immersing the ring in an expanding bubble of nothing allows to balance the forces and remove all the conical singularities.

In the following we present the metrics for these systems and prove that it is possible to achieve equilibrium configurations. A more complete analysis of the physical magnitudes and of the first law of thermodynamics for black hole systems in expanding bubbles will be the subject of future work [221].

3.3.1 4D black hole binary in equilibrium inside the expanding bubble

Superposing the rods of the 4D bubble of nothing and the Bach–Weyl binary, we get the diagram of Fig. 3.8.

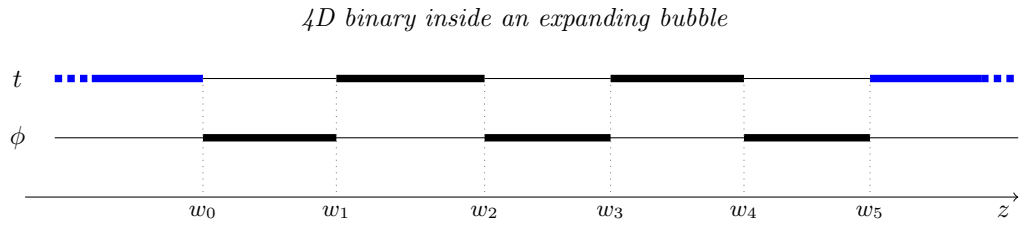

Figure 3.8: Rod diagram for a binary black hole system inside a bubble of nothing. The black timelike rods (thick lines of the t coordinate) represent the black hole horizons, while the blue timelike semi-infinite rods correspond to the bubble horizon. This diagram corresponds to the double-Wick rotation of the three-source Israel–Khan solution [139].

The solution can be written explicitly in Weyl coordinates (3.10) with

$$g_{ab}dx^a dx^b = -\rho^2 \frac{\mu_1\mu_3\mu_5}{\mu_0\mu_2\mu_4} dt^2 + \frac{\mu_0\mu_2\mu_4}{\mu_1\mu_3\mu_5} d\phi^2 \,, \tag{3.33a}$$

$$f = \frac{16 C_f\, \mu_0^5\mu_1^7\mu_2^5\mu_3^7\mu_4^5\mu_5^7}{\mu_{01}\mu_{03}\mu_{05}\mu_{12}\mu_{14}\mu_{23}\mu_{25}\mu_{34}\mu_{45} W_{02}^2 W_{04}^2 W_{13}^2 W_{15}^2 W_{24}^2 W_{35}^2 W_{00} W_{11} W_{22} W_{33} W_{44} W_{55}} \,. \tag{3.33b}$$

In the limit in which the bubble horizon is pushed to infinity, for $w_0 \to -\infty$ and $w_5 \to \infty$, we recover the standard Bach–Weyl binary (3.28). On the other hand the limit to the bubble can be obtained in different ways: by focusing on the bubbles in between black holes as we have done above, e.g.. taking $w_1 \to -\infty$ and $w_4 \to \infty$, or alternatively by eliminating the black holes by collapsing their rods, thus $w_1 = w_2 = w_3 = w_4$.

In general, the geometry contains conical singularities on the z-axis in the intervals (w_0, w_1), (w_2, w_3), and (w_4, w_5), which we eliminate by imposing (3.11) on each interval. As we mentioned, we can choose C_f (i.e. a rescaling of f) to set $\Delta\phi = 2\pi$ without loss of generality. Then, requiring (3.11) on $z \in (w_0, w_1)$ fixes

$$\begin{aligned} C_f = 2^{12} &(w_0 - w_2)^2 (w_1 - w_2)^2 (w_2 - w_3)^2 (w_0 - w_4)^2 \\ &\times (w_1 - w_4)^2 (w_3 - w_4)^2 (w_2 - w_5)^2 (w_4 - w_5)^2 \,, \end{aligned} \tag{3.34}$$

while for $z \in (w_2, w_3)$ and $z \in (w_4, w_5)$ we get

$$\frac{(w_0 - w_2)(w_2 - w_3)(w_1 - w_4)(w_2 - w_5)}{(w_0 - w_1)(w_1 - w_3)(w_2 - w_4)(w_1 - w_5)} = 1 \,, \tag{3.35a}$$

$$\frac{(w_0 - w_2)(w_0 - w_4)(w_2 - w_5)(w_4 - w_5)}{(w_0 - w_1)(w_0 - w_3)(w_1 - w_5)(w_3 - w_5)} = 1 \,. \tag{3.35b}$$

These can be solved in terms of the bubble parameters w_0 and w_5, thus leaving the binary parameters $w_{1,2,3,4}$ unconstrained. To this end, we first choose a convenient parametrization of the rod endpoints in terms of the Komar masses M_1, M_2 of the two black holes (these are half the coordinate length of the horizon rod), the coordinate distance between

them, d, and their coordinate distances to the left and right bubble horizons, ℓ_1 and ℓ_2, so that

$$w_0 = -\ell_1\,, \qquad w_1 = 0\,, \qquad w_2 = 2M_1\,, \qquad w_3 = 2M_1 + d\,, \tag{3.36a}$$

$$w_4 = 2M_1 + 2M_2 + d\,, \qquad w_5 = 2M_1 + 2M_2 + d + \ell_2\,. \tag{3.36b}$$

We then solve the equilibrium conditions (3.35) for ℓ_1 and ℓ_2, to find

$$\ell_i = \frac{\sqrt{A_i + B_i^2} - B_i}{2M_1M_2 + d(M_1 + M_2)}\,, \tag{3.37}$$

where we have defined

$$A_1 = d(d + 2M_1)(d + M_2)(d + 2(M_1 + M_2))(2M_1M_2 + d(M_1 + M_2))\,, \tag{3.38}$$

$$B_1 = d^2M_2 + 2M_1M_2(M_1 + M_2) + d(M_1^2 + 3M_1M_2 + M_2^2)\,, \tag{3.39}$$

and A_2, B_2 are obtained by changing $1 \leftrightarrow 2$. Since ℓ_1 and ℓ_2 in (3.37) are manifestly positive when M_1, M_2, d are positive, we have proven that there always exists a unique bubble, with suitably chosen position and size, that provides the necessary expansion to balance an arbitrary binary in static equilibrium (even if unstable).

It is interesting to observe that when the two black holes are very close, $d \ll M_1, M_2$, the bubble distance to them becomes

$$\ell_1, \ell_2 = d + O(d^2)\,, \tag{3.40}$$

i.e., as expected, the bubble snugly hugs the binary. When the black holes are instead far apart, $d \gg M_1, M_2$, we have

$$\ell_1, \ell_2 = \frac{d^{3/2}}{\sqrt{M_1 + M_2}}\Big(1 + O(d^{-1/2})\Big)\,, \tag{3.41}$$

which we can easily understand. The Newtonian gravitational potential between the black holes is

$$V_g \simeq -\frac{M_1 + M_2}{d}\,, \tag{3.42}$$

and the gravitational potential from the de Sitter-like expanding space between them is (for $\ell_{1,2} \simeq \ell$)

$$V_{exp} \simeq -\frac{d^2}{2\ell^2}\,, \tag{3.43}$$

since $1/\ell^2$ acts like a cosmological constant[8]. Then (3.41) follows from the equilibrium condition

$$\frac{\partial(V_g + V_{exp})}{\partial d} = 0\,. \tag{3.44}$$

[8]The two potentials can be read from g_{tt} in the weak field regime.

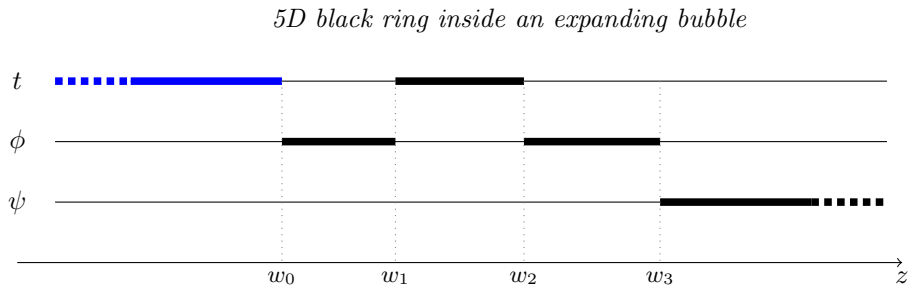

Figure 3.9: Rod diagram for the black ring inside the bubble of nothing. A semi-infinite timelike rod for $z < w_0$ has been added to the ordinary black ring diagram.

3.3.2 Black ring in equilibrium inside the expanding bubble

Now we insert a static black ring inside a five-dimensional bubble of nothing. Instead of the (x, y) coordinates used in (3.3), we will employ Weyl coordinates. For the black ring, the explicit transformation can be found in [200].

The rod diagram for the black ring is represented by the black lines in Fig. 3.9, and we add the bubble by putting an extra pole and the blue line representing the bubble horizon. Incidentally, this diagram is the double Wick-rotated version of the static black Saturn [93] (see also Fig. 3.11).

The metric corresponding to Fig. 3.9 is

$$g_{ab}dx^a dx^b = -\rho^2 \frac{\mu_1}{\mu_0\mu_2} dt^2 + \frac{\mu_0\mu_2}{\mu_1\mu_3} d\phi^2 + \mu_3 d\psi^2 \,, \tag{3.45a}$$

$$f = C_f \frac{\mu_3 W_{01}^2 W_{03} W_{12}^2 W_{23}}{W_{02}^2 W_{13} W_{00} W_{11} W_{22} W_{33}} \,. \tag{3.45b}$$

We have to eliminate conical singularities by tuning the parameters of the solution to satisfy (3.11) at every spacelike rod. If we choose $\Delta\psi = 2\pi$, we find that (3.11) is satisfied along the segment $z \in (w_3, \infty)$ by setting $C_f = 1$. Next, imposing (3.11) on the ϕ direction along $z \in (w_0, w_1)$ and along $z \in (w_2, w_3)$, we obtain

$$\frac{(w_1 - w_0)^2 (w_3 - w_0)}{(w_2 - w_0)^2} = \frac{1}{2} \left(\frac{\Delta\phi}{2\pi} \right)^2 \,, \tag{3.46a}$$

$$\frac{(w_3 - w_0)(w_3 - w_2)}{w_3 - w_1} = \frac{1}{2} \left(\frac{\Delta\phi}{2\pi} \right)^2 \,. \tag{3.46b}$$

In order to solve these equations, we parametrise the rod endpoints as

$$w_0 = -\ell \,, \qquad w_1 = 0 \,, \qquad w_2 = 2\mu R^2 \,, \qquad w_3 = (1+\mu) R^2 \,. \tag{3.47}$$

Here ℓ characterizes the bubble size, while $\mu \in [0, 1)$ and R are the same parameters for the shape and radius of the ring as in (3.3). Eqs. (3.46) are solved with

$$\ell = R^2 \left(1 - \mu + \sqrt{1 - \mu^2} \right) , \tag{3.48}$$

and[9]

$$\left(\frac{\Delta\phi}{2\pi}\right)^2 = 2R^2\left(2+\sqrt{1-\mu^2}\right)\frac{1-\mu}{1+\mu}\,. \tag{3.49}$$

Thus, we can always choose, in a unique way, the bubble size ℓ so as to balance into equilibrium an arbitrary static black ring.

To finish this section, we shall mention that, with a straightforward exercise in rodology, which we leave to the reader, one can insert the five-dimensional binary of Fig. 3.7(a) inside the bubble of Fig. 3.7(b), and then obtain the corresponding solution (which is a limit of the ones in [220]). Given our previous analyses, it is natural to expect, and consistently with parameter counting, that the bubble parameters can be adjusted to balance an arbitrary binary of this kind.

3.4 Other configurations

We can extend the discussion of the previous sections to more general configurations, and play with the rods to move from one solution to another. There are plenty of examples that can be considered, both in four and five dimensions, and even in higher dimensions [200]. We will consider some of them, just to give a taste of the many possibilities that are offered by the rod diagram machinery. The limits presented below on the rods diagrams work faithfully on the corresponding metrics.

3.4.1 Four dimensions

One obvious extension of the binary system studied above is the three-black hole configuration contained in the Israel–Khan solution and represented in Fig. 3.10(a). To get the Schwarzschild black hole inside the bubble of nothing, we extend the peripheral timelike rods to infinity, taking the limits $w \to -\infty$ and $w_5 \to \infty$.

From the black hole in the bubble we can also generate a metric describing a point-like Curzon–Chazy particle embedded in the bubble. The procedure is similar to the one used to obtain the Bonnor–Swaminarayan solution from an accelerating binary black hole system [151].

Moreover it is very clear, in the 4D setting, how to generate accelerating black hole metrics from the black holes in the bubble, for any number of collinear black holes. It is sufficient to push away only one of the two poles defining the bubble, for instance $w_0 \to -\infty$ in the binary configuration of Sec. 3.3.1. In Fig. 3.10 we picture the single black hole case. The limiting process, however, introduces irremovable conical singularities, unless an external background field is introduced, as in [151]. It is clear that this procedure cannot be pursued in 5D. In that case, there is only a single rod determining the bubble horizon, but more importantly, the five-dimensional C-metric for a uniformly accelerating black hole would have different symmetry ($SO(3)$ rotations, rather than $U(1)^2$) and not be in the Weyl class of solutions.

[9] We could absorb a scale $\propto R$ in the definition of ϕ to make it dimensionless, as we have done before.

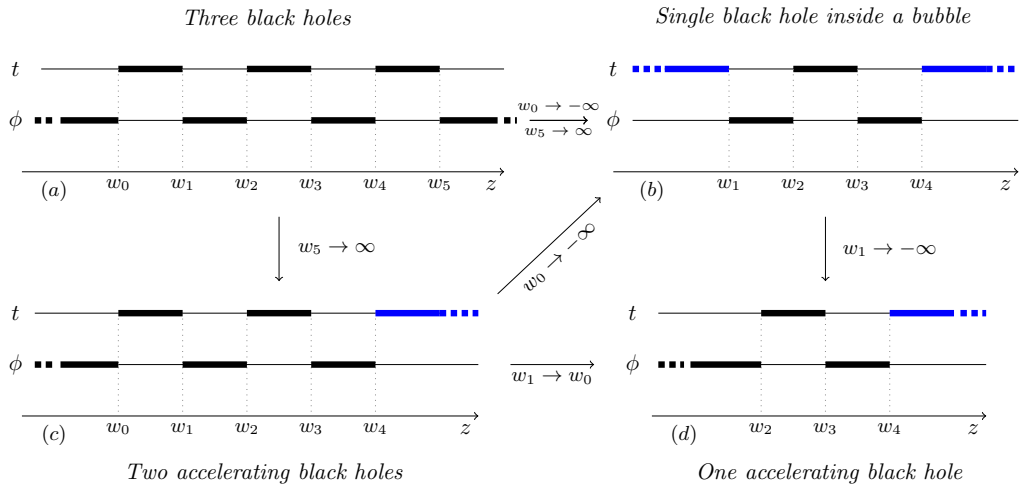

Figure 3.10: (a) Rod diagram for a collinear three-black hole system (an Israel–Khan solution). The limit $w_0 \to -\infty$ and $w_5 \to \infty$ gives (b) the single black hole in the expanding bubble. When sending $w_5 \to \infty$ in (a) we obtain (c) two accelerating black holes. Collapsing one timelike rod in the latter gives (d) the C-metric for a single accelerating black hole. The rod limits commute, so from the two accelerating black holes in (c), the limit $w_0 \to -\infty$ gives (b) a single black hole in a bubble.

3.4.2 Five dimensions

It is interesting that all the five-dimensional configurations studied in this paper can be obtained by performing limits in the black di-ring configuration of Fig. 3.11(a).

For instance, to recover the black ring-bubble of nothing of Fig. 3.11(b) (which also corresponds to Fig. 3.9), we simply send $w_1 \to -\infty$ in the black di-ring diagram. Furthermore, one can also obtain the black hole inside the bubble from the latter by taking $w_5 \to w_4$ to remove a spacelike finite rod.

On the other hand, if we take $w_5 \to w_4$ in the di-ring diagram, we recover the black Saturn [93] of Fig. 3.11(c). From this diagram, we can send $w_1 \to -\infty$ to obtain the 5D black hole-bubble of nothing, which corresponds to the superposition of the two diagrams of Fig. 3.4.

3.5 Outlook

Black holes and bubbles of nothing are some of the most elementary solutions in General Relativity, and in this chapter we have argued that their properties are closely interrelated. By revealing how bubbles are present in black hole systems, we have learned that the spacetime expansion in the bubble is driven by the same phenomenon that makes the volume inside a black hole grow.

The basic idea is simple enough to lend itself to easy generalization. Whenever a

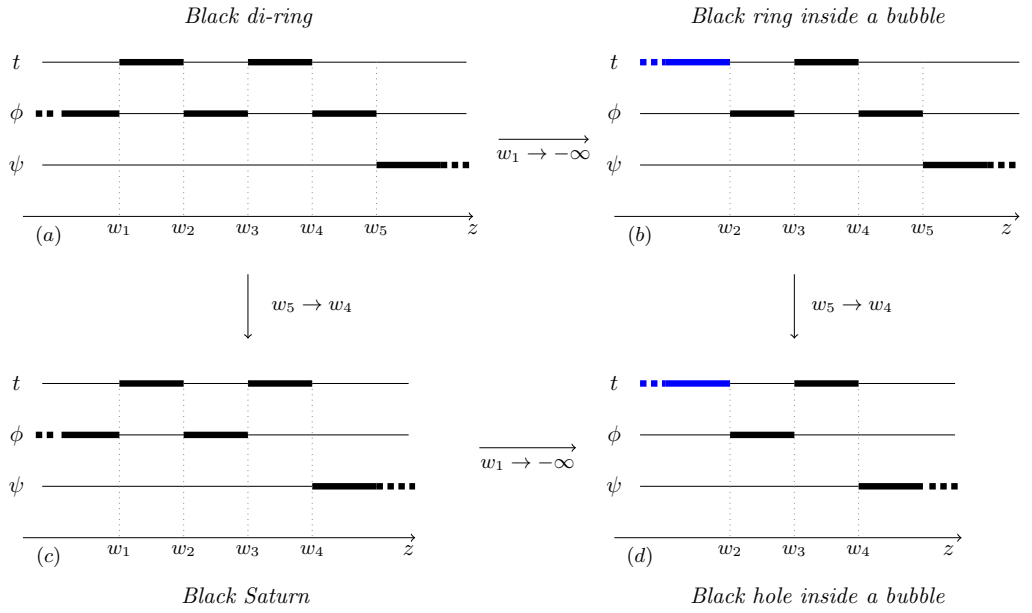

Figure 3.11: (a) Rod diagram for a coaxial double black ring system. The limit $w_1 \to -\infty$ gives (b) the single black ring in the expanding bubble. The limit of (a) for $w_5 \to w_4$ gives (c) the black Saturn. Its limit for $w_1 \to -\infty$ gives (d) the five-dimensional black hole in an expanding bubble. The rod limits commute, so the latter diagram can also be obtained from (b) for $w_5 \to w_4$.

small gap region appears between black hole horizons in a maximally extended geometry, it will contain an expanding bubble of nothing. The bubble is a minimal cycle that links the Einstein–Rosen bridges of the system. In the simplest instance, namely, the four-dimensional black hole binary in Sec. 3.2.3, the topology of a Cauchy slice is $S^1 \times S^2 - \{0\}$ (the point at infinity is removed), and the bubble is the minimal S^1 in it. Similarly, for the black ring, the spatial topology is $S^2 \times S^2 - \{0\}$, and the bubble is the minimal S^2. In the more general "ringoids" of [213, 214] with spatial topology $S^{d-3} \times S^2 - \{0\}$ we find S^{d-3} bubbles. We have even considered more complex bubbles topologies, such as the double S^2 bubble in Sec. 3.2.5, and we have identified that a collinear black hole binary in d dimensions, with Cauchy slices that are $S^1 \times S^{d-2} - \{0\}$, must have an S^1 bubble.

Such solutions for binary black holes are not known explicitly in arbitrary dimensions, but we can easily find configurations with two disconnected horizons which can be regarded, in the sense explained above, as possessing expanding bubbles of nothing. The Schwarzschild–de Sitter solution

$$ds^2 = -\left(1 - \frac{\mu}{r^{d-3}} - \frac{r^2}{L^2}\right)dt^2 + \frac{dr^2}{1 - \frac{\mu}{r^{d-3}} - \frac{r^2}{L^2}} + r^2 d\Omega_{d-2}\,, \tag{3.50}$$

with

$$0 < \mu < \mu_N \equiv \frac{2}{d-3}\left(\frac{d-3}{d-1}\right)^{\frac{d-1}{2}} L^{d-3}\,, \tag{3.51}$$

has a cosmological horizon and a black hole horizon. In the maximal analytic extension (and identifying regions beyond the horizons to form a spatial circle) the spatial sections have topology $S^1 \times S^{d-2}$. The S^1 expands in time, inside the black hole and in the time-dependent region beyond the de Sitter horizon. The analogue of the bubble limit is the limit $\mu \to \mu_N$, in which (after rescaling t) we recover the Nariai solution

$$ds^2 = \frac{L^2}{d-1}\left[-(1-\xi^2)dt^2 + \frac{d\xi^2}{1-\xi^2} + (d-3)d\Omega_{d-2}\right], \tag{3.52}$$

with horizons at $\xi = \pm 1$. We can change coordinates in this metric (see footnote 3) to the form

$$ds^2 = \frac{L^2}{d-1}\left[-dT^2 + \cosh^2 T d\chi^2 + (d-3)d\Omega_{d-2}\right], \tag{3.53}$$

with $0 \leq \chi \leq 2\pi$. Here we recognise the essential features of the $n = 1$ circular bubble (3.1), only that now the inhomogeneous, non-compact (r, ϕ) cigar is replaced by a round S^{d-2}. Thus, bubble-of-nothing-like expansion is indeed pervasive and connected in wide generality to the phenomenon of spacetime expansion.

It is now clear, given the plethora of black hole topologies and multi-black hole configurations that are possible in higher dimensions [222], that we can expect a large variety of expanding bubbles of nothing, even in vacuum gravity. Many of them are unlikely to admit a closed exact solution, but it is intuitively useful to first conceive of them as black hole configurations, as this helps identify new possibilities. It would be interesting

to know how general the converse is, that is, whether for any expanding bubble one can find a black hole configuration that contains it as a limit.

We have also proven, with explicit examples, that the bubble expansion acts on gravitating systems in much the same way as de Sitter-type inflation: it counteracts the gravitational attraction between localized objects and allows novel static multi-black hole configurations. Again, this phenomenon is likely valid for all the expanding bubbles that we have mentioned above, and more generally for other bubbles.

Our arguments show that the expanding bubble of nothing is already present in the binary or black ring *even before taking the small-gap limit*, in the sense that there is a minimal cycle that links the system of Einstein–Rosen bridges and which expands because it stretches inside the black holes. Taking the small-gap limit makes the bubble more symmetric and uniform, and its expansion becomes asymptotically uniform and eternal, since in the limit the interior black hole singularity is pushed away to infinitely late time. If the black hole system were of finite size, or if it were to merge or collapse, the duration of the expansion would instead be limited, ending on a singularity. But expanding bubbles of nothing, in the above sense, seem pervasive in black hole systems with multiple or non-spherical horizons[10].

Does this mean that we should expect bubbles of nothing in astrophysical, dynamical binaries more realistic than the static ones we have studied? Unfortunately, the answer is no. The topology of a binary where the black holes formed from collapsing matter is different than in the maximal analytic extensions we have considered. Collapsing black hole geometries do not have bifurcation surfaces nor Einstein–Rosen bridges. Even though space expands inside a collapsing black hole, the topology of the Cauchy slices is trivial, and these binaries will not contain any minimal cycle.

However, even if expanding bubbles of nothing may not be present in the sky above, their connection to more conventional black hole systems provides a new, illuminating perspective on their properties and makes them seem more accessible. Since they behave in many ways like de Sitter space, but without a cosmological constant, and with non-compact horizons, they may provide new venues in which to investigate the holographic description of expanding spacetime, possibly exploiting their relation to Einstein–Rosen bridges and the interiors of black hole systems.

[10] However, this does not mean that they must admit a good limit to a bubble solution; we already mentioned in Sec. 3.2.1 that the equilibrium rotating black ring does not admit it, even though at any finite radius it has a bubble in the sense explained above.

CHAPTER 4

Black holes in a swirling universe

In this Chapter we will explore the "magnetic" version of the Ehlers transformation presented in Sec. 1.1 in the context of vacuum General Relativity. The effect of such a symmetry map has not been investigated until now, at best of our knowledge. Actually, the spacetime resulting from the application of the modified Ehlers map to the Minkowski metric was presented in an Appendix of [223], but it was not studied and its physical properties were not unraveled.

The purpose of this Chapter is to investigate the last unexplored Lie point symmetry of the $SU(2,1)$ group and to explore the properties of the spacetime that it generates. We will see that such a transformation embeds any given stationary and axisymmetric seed spacetime into a rotating background, which we will dub "swirling universe", for its peculiar characteristic. Indeed, the background can be interpreted as a gravitational whirlpool, and its frame dragging turns a static seed solution into a stationary metric. The resulting spacetime really looks similar to the Taub–NUT metric, however we will show that it does not share the problematic features of its "electric" counterpart: in fact, our new spacetime does not possess any Misner string, nor is affected by the presence of conical singularities. The manifold is completely regular, apart from the presence of the usual black hole curvature singularity.

Firstly, we generate the new metric via the "magnetic" Ehlers map. Then, we test the consequences of the transformation on the spherical symmetric black hole, which will be our seed metric, as done with the symmetries previously analysed in the literature. In this way we generate a novel and analytic exact solution of the Einstein equations, which generalises and deforms the Schwarzschild spacetime. Of course, because of the well-known no-hair theorems for black hole in four-dimensional General Relativity, the new solution can be a black hole only by renouncing to asymptotic flatness, similarly to black holes embedded in the external electromagnetic field of Melvin universe [130, 117, 223]. We also present the generalisation to the Kerr black hole in the rotating background. Finally, we conclude the Chapter by establishing a connection (via a double-Wick rotation) between our background metric and the flat Taub–NUT spacetime. This Chapter is based on [224].

4.1 Generation of the solution

As explained above, we consider the magnetic LWP metric of Eq. (1.48),

$$ds^2 = \bar{f}(d\varphi - \bar{\omega}dt)^2 + \bar{f}^{-1}\left[e^{2\bar{\gamma}}\left(d\rho^2 + dz^2\right) - \rho^2 dt^2\right], \tag{4.1}$$

and the Ehlers transformation (1.46c)

$$\mathcal{E}' = \frac{\mathcal{E}}{1 + i\jmath\mathcal{E}}, \tag{4.2}$$

where we dubbed with $\jmath$ the map parameter.

First of all we have to choose the seed. We start with the Schwarzschild black hole, whose metric, in spherical coordinates, reads

$$ds^2 = -\left(1 - \frac{2m}{r}\right)dt^2 + \frac{dr^2}{1 - \frac{2m}{r}} + r^2 d\theta^2 + r^2 \sin^2\theta d\varphi^2 . \tag{4.3}$$

The most convenient coordinates for the generating methods, in this case, are the spherical ones (r, θ), related to the Weyl cylindrical coordinates by

$$\rho = \sqrt{r^2 - 2mr}\sin\theta , \quad z = (r - m)\cos\theta . \tag{4.4}$$

The line element of the LWP metric (1.48) in spherical coordinates reads

$$ds^2 = \bar{f}(d\varphi - \bar{\omega}dt)^2 + \bar{f}^{-1}\left[-\rho^2 dt^2 + e^{2\bar{\gamma}}(r^2 - 2mr + m^2\sin^2\theta)\left(\frac{dr^2}{r^2 - 2mr} + d\theta^2\right)\right]. \tag{4.5}$$

Comparing the seed (4.3) to the above metric we can identify the seed structure functions

$$\bar{f}(r, \theta) = r^2 \sin^2\theta , \quad \bar{\omega}(r, \theta) = 0 . \tag{4.6}$$

The value of $\bar{\gamma}$ is not fundamental because it is invariant under Ehlers transformations, however we explicit it for completeness

$$\bar{\gamma}_0(r, \theta) = \frac{1}{2}\log\left(\frac{r^4 \sin^2\theta}{r^2 - 2mr + m^2\sin^2\theta}\right). \tag{4.7}$$

From definition of χ in (1.33), it is clear that $\bar{\chi}$ is at most constant, but that constant can be reabsorbed via a coordinate transformation. Therefore without loss of generality we can choose $\bar{\chi} = 0$. Finally, the seed Ernst gravitational potential takes the form

$$\mathcal{E}(r, \theta) = \bar{f}(r, \theta) . \tag{4.8}$$

The new solution, expressed in terms of the complex potential, is generated via the Ehlers transformation (4.2), which gives

$$\mathcal{E}' = \frac{\mathcal{E}}{1 + i\jmath\mathcal{E}} = \frac{r^2 \sin^2\theta}{1 + i\jmath\, r^2 \sin^2\theta} . \tag{4.9}$$

Note that in case we had used the LWP metric defined in (1.7), we would had obtained, via the Ehlers transformation acting on the Schwarzschild seed, the Taub–NUT spacetime, as explained in Chapter 1.

The solution, in metric form, is extracted from the definition of the transformed Ernst potential $\mathcal{E}$. Hence, according to $\mathcal{E} = f + i\chi$, we find

$$f(r,\theta) = \frac{r^2 \sin^2\theta}{1 + \jmath^2 r^4 \sin^4\theta}\,, \qquad \chi(r,\theta) = \frac{\jmath\, r^4 \sin^4\theta}{1 + \jmath^2 r^4 \sin^4\theta}\,. \tag{4.10}$$

ω has to be found from the definition of χ, as in (1.33). The result is

$$\omega(r,\theta) = 4\jmath(r-2m)\cos\theta + \omega_0\,, \tag{4.11}$$

where ω_0 is an integration constant related to the choice of reference frame. Thus, recalling that γ is not affected by the Ehlers map, the full new metric is

$$\begin{aligned} ds^2 = F(r,\theta)\left[-\left(1-\frac{2m}{r}\right)dt^2 + \frac{dr^2}{1-\frac{2m}{r}} + r^2 d\theta^2\right] \\ + \frac{r^2\sin^2\theta}{F(r,\theta)}\left\{d\varphi + \left[4\jmath(r-2m)\cos\theta + \omega_0\right]\,dt\right\}^2\,, \end{aligned} \tag{4.12}$$

where we have defined the function

$$F(r,\theta) \coloneqq 1 + \jmath^2 r^4 \sin^4\theta\,, \tag{4.13}$$

We can immediately observe that the new metric (4.12) represents a non-asymptotically flat deformation of the Schwarzschild black hole. Its structure is quite similar to the Schwarzschild–Melvin spacetime [117], and indeed the magnetic Ehlers map that we have used works in a similar fashion as the Harrison transformation. For this reason we do not expect that the new parameter can be considered as hair nor as conserved charge of the black hole. The physical description of (4.12) will be analysed in detail in the next Section.

Starting with a more general seed we can obtain generalisations of the metric built above. In Sec. 4.4 we embed the Kerr black hole in the swirling background, while in Appendix D we generate the Zipoy–Voorhees extension of the spacetime (4.12).

4.2 Analysis of the background spacetime

In the interpretation of the new spacetime (4.12), a fundamental point comes from the physical meaning of the new parameter $\jmath$, which defines the behaviour of the gravitational background and, at best of our knowledge, is unknown. Thus, we firstly analyse the background metric obtained by turning off the mass parameter m in Eq. (4.12) and then, in Sec. 4.3, we study the full black hole solution in his surrounding universe.

When the mass parameter m vanishes the black hole disappears and we are left with the rotating gravitational background only

$$ds^2 = F\big(-dt^2 + dr^2 + r^2 d\theta^2\big) + F^{-1} r^2 \sin^2\theta (d\varphi + 4\jmath\, r\cos\theta\, dt)^2\,. \tag{4.14}$$

In cylindrical coordinates

$$\rho = r\sin\theta\,, \quad z = r\cos\theta\,, \tag{4.15}$$

the background takes the simpler form

$$ds^2 = \big(1+\jmath^2\rho^4\big)\big(-dt^2+d\rho^2+dz^2\big) + \frac{\rho^2}{1+\jmath^2\rho^4}(d\varphi+4\jmath z dt)^2\,. \tag{4.16}$$

Such a metric has the very same form as the one presented in Appendix C of [223]: however, it was not studied in that reference.

The spacetime (4.16) is characterised by the Killing vectors

$$\partial_t\,, \quad \partial_\varphi\,, \quad z\partial_t + t\partial_z - 2\jmath\big(t^2+z^2\big)\partial_\varphi\,, \quad \partial_z - 4\jmath t\partial_\varphi\,, \tag{4.17}$$

and by the Killing–Yano form

$$-4\jmath\rho z\, dt\wedge d\rho + \jmath\rho^2\big(1+\jmath^2\rho^4\big)\, dt\wedge dz + \rho\, d\rho\wedge d\varphi\,. \tag{4.18}$$

It belongs to the Petrov type D class [119], and its Newman–Penrose spin coefficient is equal to zero: these features allow us to infer that the metric (4.16) belongs to the Kundt class (cf. Table 38.9 of [119]). We can indeed explicitly express the background metric (4.16) in the standard Kundt form, by performing the rescaling $t \to \jmath t$ and the change of coordinates

$$q = 2\jmath z\,, \quad p = \rho^2\,. \tag{4.19}$$

Metric (4.16) then boils down to (after a rescaling of the conformal factor)

$$ds^2 = (\gamma^2+p^2)\big(-dt^2+dq^2\big) + \frac{\gamma^2+p^2}{\gamma^2 p}dp^2 + \frac{\gamma^2 p}{\gamma^2+p^2}(d\varphi+2\gamma q dt)^2\,, \tag{4.20}$$

where we have defined $\gamma = 1/\jmath$. This metric is equivalent to (16.27) of [135], once we put $m = e = g = \Lambda = \alpha = \epsilon_2 = k = 0$, $\epsilon_0 = 1$ and $n = \gamma^2/2$. One can check that the consistency constraints of [135] are indeed satisfied.

The metric (4.20), despite being known for a long time (it was discovered by Carter in [225]), does not have a clear physical interpretation. In particular, the physical significance of the parameter γ (i.e. $\jmath$) is unknown: it has been called "anti-NUT" parameter by Plebański in [226] because of its resemblance with the NUT parameter in the Plebański–Demiański spacetime [134][1]. A generalisation in the presence of the cosmological constant and some possible interpretations of this background are given in Sec. 4.5.

An interesting limit is given by $p \to \infty$: by putting $\gamma = 0$ after the rescaling $t \to \gamma^{-2/3}t$, $q \to \gamma^{-2/3}q$, $\varphi \to \gamma^{-2/3}\varphi$ and $p \to \gamma^{2/3}p$, one finds

$$ds^2 = p^2\big(-dt^2+dq^2\big) + p\, dp^2 + \frac{1}{p}d\varphi^2\,. \tag{4.21}$$

This is nothing but the Levi-Civita metric [227] (cf. (10.9) of [182]), in the limiting case when $\sigma = 1/4$, which is locally isometric to the asymptotic form of the Melvin spacetime,

[1] Actually, there exists a connection between the rotating parameter $\jmath$ and the NUT parameter ℓ that will be exploited in Sec. 4.5.

as shown in [228, 189, 229]; another connection to the magnetic universe will be explored in Sec. 4.5. Finally, the above limit can also be expressed in the Kasner-like form [230].

In order to gain some physical perspective is useful to investigate, in some detail, the properties of the background metric by inspecting its geodesics.

4.2.1 Geodesics in the background spacetime

We define the following geodesic Lagrangian from the background metric (4.16)

$$\mathscr{L} = \left(1 + \jmath^2\rho^4\right)\left(-\dot{t}^2 + \dot{\rho}^2 + \dot{z}^2\right) + \frac{\rho^2}{1+\jmath^2\rho^4}\left(\dot{\varphi} + 4\jmath z\dot{t}\right)^2 , \tag{4.22}$$

where the dots stand for the derivatives with respect to an affine parameter s. We can define, via the Killing vectors $\xi = \partial_t$ and $\Phi = \partial_\varphi$, the standard conserved quantities

$$-E \coloneqq g_{\mu\nu}u^\mu\xi^\nu , \quad L \coloneqq g_{\mu\nu}u^\mu\Phi^\nu , \tag{4.23}$$

where u^μ is the four-momentum of the test particle, E is the energy and L is the angular momentum. The explicit definitions for the conserved quantities and the resulting Lagrangian can be found in Appendix C.1

The equations of motion derived from the Lagrangian are quite involved. Qualitative results can be obtained from the normalisation of the four-momentum, i.e. from equation $u^\mu u_\mu = \chi$, with $\chi = -1$ for timelike geodesics and $\chi = 0$ for null geodesics. The resulting normalisation equation is (C.3). For large values of ρ and for fixed z, it follows from such equation that

$$\dot{\rho}^2 \approx L^2\rho^{-2} , \tag{4.24}$$

which has solution $\rho(s) \propto \sqrt{2Ls}$: this means that ρ is not limited as the affine parameter grows.

We are interested in analysing the behaviour of z as ρ grows. We find $\dot{z}^2 = 0$ by letting $\rho \to \infty$ in equation (C.3), therefore the coordinate z reaches a constant value as ρ approaches infinity. Moreover, the equation defining L, for large values of ρ, gives $\phi \approx c^2L^2s^2$. Combining this with the approximate equation for ρ, allows one to get the polar equation $r \approx \sqrt{\frac{2}{c}}\phi^{1/4}$. Such an equation is the polar form of the generalised Archimedean spiral with exponential $1/4$. Therefore we expect that a geodesic test particle follows a spiral-like path in the (x, y) plane and that it moves toward a constant value of z. These results are in good agreement with the numerical evaluations, as can be observed from the plot in Fig. 4.1, which shows the trajectory of a test particle in the (x, y, z) space, where $x = \rho\cos\theta$, $y = \rho\sin\theta$.

The statement that z reaches a constant value can be verified by using the equation of motion for z

$$4\jmath^2\rho^3\dot{\rho}\dot{z} + (\jmath^2\rho^4 + 1)\ddot{z} = \frac{4\rho^2\jmath\dot{t}(\dot{\varphi} + 4\jmath z\dot{t})}{\jmath^2\rho^4 + 1} . \tag{4.25}$$

By inspecting the equations for $\dot{t}$ and $\dot{\varphi}$ in Appendix C.1, one can notice that $\dot{t} \propto 1/\rho^4$ and $\dot{\varphi} \propto \rho^2$ as $\rho \to \infty$, therefore the r.h.s. of the latter equation can be neglected for large

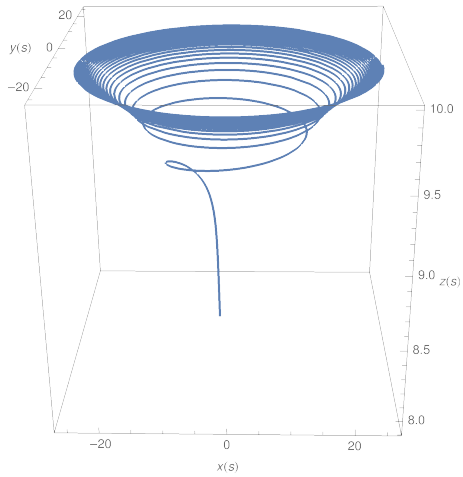

Figure 4.1: Geodesic motion of a test particle in the gravitational background for $E = 1$, $L = 1$, $\jmath = 0.1$.

values of ρ:

$$4\jmath^2\rho^3\dot{\rho}\dot{z} + (\jmath^2\rho^4 + 1)\ddot{z} = 0\,. \tag{4.26}$$

Moreover, $1 + \jmath^2\rho^4 \approx \jmath^2\rho^4$ as ρ approaches infinity. By using the approximation $\rho(s) \approx \sqrt{2Ls}$ found above, the equation becomes

$$2\dot{z} + s\ddot{z} = 0\,, \tag{4.27}$$

whose solution is

$$z(s) = \frac{D}{s} + C\,, \tag{4.28}$$

where C, D are integration constants. This result clearly shows that z becomes constant as s approaches infinity.

4.3 Schwarzschild black hole in a swirling universe

4.3.1 Physical properties

The full black hole metric (4.12), that we report here for convenience

$$\begin{aligned} ds^2 = F(r,\theta)\left[-\left(1-\frac{2m}{r}\right)dt^2 + \frac{dr^2}{1-\frac{2m}{r}} + r^2 d\theta^2\right] \\ + \frac{r^2\sin^2\theta}{F(r,\theta)}\left\{d\varphi + \left[4\jmath(r-2m)\cos\theta + \omega_0\right]dt\right\}^2, \end{aligned} \tag{4.29}$$

with $F(r,\theta) = 1 + \jmath^2 r^4 \sin^4\theta$, is a two parameters metric, with m and $\jmath$ related to the mass of the black hole and the angular velocity of the background, respectively.

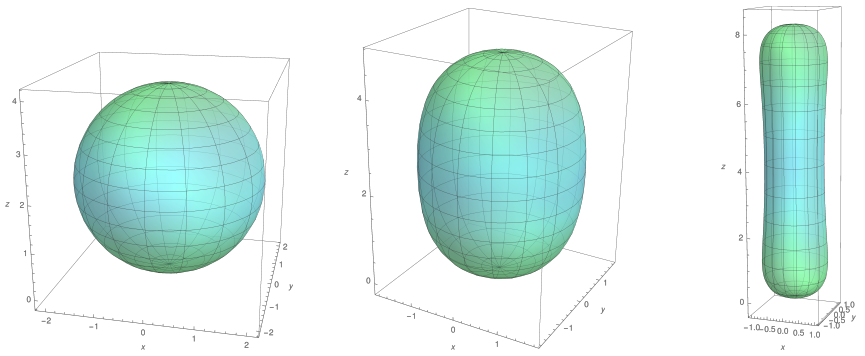

(a) $m = 1, \jmath = 0.05$ (b) $m = 1, \jmath = 0.1$ (c) $m = 1, \jmath = 0.3$

Figure 4.2: Embedding in Euclidean three-dimensional space $\mathbb{E}^3$ of the event horizon of the black hole distorted by the rotating background, for three different values of the background rotational parameter $\jmath$.

In view of the previous Section, the spacetime (4.29) can be interpreted as a Schwarzschild black hole embedded into a swirling background. The main casual structure is similar to the Schwarzschild case, as can be readily understood by looking at some $\theta =$ constant slices of the conformal diagram. For instance, the cases $\theta = \{0, \pm\pi\}$ precisely retrace the static spherically symmetric black hole.

Indeed the metric (4.29) is characterised by a coordinate singularity located at $r = 2m$, which identifies the event horizon of the black hole. This latter is a Killing horizon that has the same significance of the standard Schwarzschild horizon. The presence of the rotating background deforms the horizon geometry, making it more oblate, while maintaining exactly the same of the Schwarzschild black hole, for the same values of the mass parameter m. In Fig. 4.2 the deformation is pictured for different intensities of the rotating gravitational background, governed by the new parameter $\jmath$ introduced by the Ehlers transformation.

The solution (4.29) is free from axial conical singularities: to verify this, it is sufficient to consider the ratio between the perimeter of a small circle around the z-axis, both for $\theta = 0$ and $\theta = \pi$, and its radius. Such a ratio must be equal to 2π, in case one wants to avoid angular defects. It turns out that, for the metric (4.29), the ratios in the two limits are equal to 2π

$$\lim_{\theta\to 0} \frac{1}{\theta} \int_0^{2\pi} \sqrt{\frac{g_{\varphi\varphi}}{g_{\theta\theta}}} d\varphi = 2\pi = \lim_{\theta\to\pi} \frac{1}{\pi - \theta} \int_0^{2\pi} \sqrt{\frac{g_{\varphi\varphi}}{g_{\theta\theta}}} d\varphi \,. \tag{4.30}$$

The metric function $\omega(r, \theta)$ is regular both asymptotically and on the symmetry axis, thus implying the absence of Misner strings or NUT charges. It is not only continuous, as we can appreciate by the following limits

$$\lim_{\theta\to 0} \frac{g_{t\varphi}}{g_{tt}} = \lim_{\theta\to\pi} \frac{g_{t\varphi}}{g_{tt}} = 0 \,, \tag{4.31}$$

but also its first and second derivatives are continuous.

A peculiar characteristic of this metric is that the angular velocity Ω on the z-axis is not constant, and it increases in opposite directions in the two hemispheres

$$\Omega\big|_{\theta=0} = \lim_{\theta\to 0}\left(-\frac{g_{t\varphi}}{g_{\varphi\varphi}}\right) = -4\jmath(r-2m)+\omega_0\,, \tag{4.32a}$$

$$\Omega\big|_{\theta=\pi} = \lim_{\theta\to \pi}\left(-\frac{g_{t\varphi}}{g_{\varphi\varphi}}\right) = 4\jmath(r-2m)+\omega_0\,. \tag{4.32b}$$

This is a feature shared with magnetised Reissner–Nordström and magnetised Kerr black holes solutions [223].

The frame dragging of the whole spacetime is given by [231]

$$\frac{d\phi}{dt} = -\frac{g_{t\varphi}}{g_{\varphi\varphi}} = -4\jmath(r-2m)\cos\theta+\omega_0\,. \tag{4.33}$$

Hence, outside the event horizon, for $r > 2m$, the angular velocity coincides with the asymptotic one ω_0 for $\theta = \frac{\pi}{2}$, while for $\theta \in (\frac{\pi}{2}, \pi)$ it is bigger than ω_0 and for $\theta \in (0, \frac{\pi}{2})$ it is smaller than ω_0. It is easy to verify that for $r \to \infty$ the angular velocity grows unbounded and that it is equal to ω_0 on the event horizon: this would lead to the conclusion that superluminal observers exist, since the value of the gravitational dragging can easily exceed 1 (i.e. the speed of light, in our units) and, then, it would violate causality. In this perspective, let us study the possible occurrence of closed timelike curves (CTCs): considering (4.29), curves in which t, r and θ are constants are characterised by

$$ds^2_{t,r,\theta=\text{const}} = F^{-1}(r,\theta)\, r^2\sin^2\theta d\phi^2\,. \tag{4.34}$$

Such intervals are always space-like since the expression is always positive. Therefore there are no CTCs and there are no related causality issues: thus the "paradox" of the superluminal observers can be justified with the bad choice of the coordinates[2]. A set of coordinates which is adapted to timelike observers does not experience an unbounded growth of the angular velocity, as we will see explicitly when studying the geodesics of the spacetime.

The Kretschmann scalar $R_{\mu\nu\rho\sigma}R^{\mu\nu\rho\sigma}$ suggests that $r = 2m$ is a coordinate singularity, while it is divergent for $r = 0$, as in the case of the static spherically symmetric black hole in pure General Relativity. It is indeed possible to find an Eddington–Finkelstein coordinate system that removes the $r = 2m$ horizon. In particular, as $r \to 0$ we find

$$R_{\mu\nu\rho\sigma}R^{\mu\nu\rho\sigma} \approx \frac{48m^2}{r^6}\,, \tag{4.35}$$

which is exactly the Kretschmann scalar for the Schwarzschild spacetime. On the other hand, the scalar invariant falls faster than the Schwarzschild metric for large radial distances, indeed one finds, as $r \to \infty$,

$$R_{\mu\nu\rho\sigma}R^{\mu\nu\rho\sigma} \approx \frac{192}{\jmath^4\sin^{12}\theta\, r^{12}}\,, \tag{4.36}$$

[2] As it happens, for example, for the Alcubierre spacetime [232]

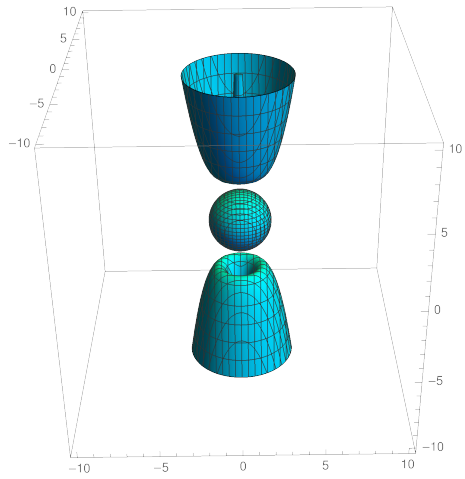

Figure 4.3: Ergoregions for the black hole embedded in a rotating universe, with parameters $m = 1$, $\jmath = 0.3$ and $\omega_0 = 0$. The ergoregions extend to infinity in the positive and negative z directions, independently of the choice of the parametrisation for the integrating constants.

therefore the solution (4.29) is locally asymptotically flat. We finally notice that for $\theta = 0, \pi$ the spacetime has an asymptotically constant curvature: we find

$$R_{\mu\nu\rho\sigma}R^{\mu\nu\rho\sigma}\big|_{\theta=0,\pi} \approx -192\jmath^2 \quad \text{as } r \to \infty\,, \tag{4.37}$$

thus we see that on the z-axis, the spacetime is asimptotically of negative constant curvature.

4.3.2 Ergoregions

It is clear, just by inspection, that the g_{tt} component of the metric (4.29) becomes null on the event horizon, and that outside the horizon is not everywhere negative. Therefore the spacetime presents some ergoregions, analogously to Kerr or magnetised Reissner–Nordström black holes [223]. To analyse these regions it is convenient to use the cylindrical coordinates as defined in (4.15) to expand, for large z, the g_{tt} part of the metric as follows

$$g_{tt}(\rho, z) \approx \frac{16\jmath^2\rho^2 z(z-4m)}{1+\jmath^2\rho^4}\,. \tag{4.38}$$

Hence, the ergoregions are located not only in the proximity of the event horizon, as in Kerr spacetime, but also close to the z-axis, for large values of z. A numerical analysis of the function g_{tt} is represented in Fig. 4.3: it shows how the ergoregions extend to infinity around the polar axis, independently of the values of the integrating constants of the solution $(m, \jmath)$. This behaviour is similar to what happens for magnetised rotating black holes [223].

4.3.3 Petrov type

A standard procedure to determine the Petrov type of a spacetime consists in computing the Weyl tensor in a null tetrad basis. We define a frame by

$$e^0 = F^{1/2}\left(1-\frac{2m}{r}\right)^{1/2} dt\,, \tag{4.39a}$$

$$e^1 = F^{1/2}\left(1-\frac{2m}{r}\right)^{-1/2} dr\,, \tag{4.39b}$$

$$e^2 = rF^{1/2}\,d\theta\,, \tag{4.39c}$$

$$e^3 = r\sin\theta F^{-1/2}\left\{d\varphi + \left[4\jmath(r-2m)\cos\theta + \omega_0\right]\,dt\right\}. \tag{4.39d}$$

Given such a frame, the null tetrad is found as

$$k_\mu = \frac{1}{\sqrt{2}}\left(e^0_\mu + e^3_\mu\right), \quad l_\mu = \frac{1}{\sqrt{2}}\left(e^0_\mu - e^3_\mu\right), \quad m_\mu = \frac{1}{\sqrt{2}}\left(e^1_\mu - ie^2_\mu\right), \quad \bar{m}_\mu = \frac{1}{\sqrt{2}}\left(e^1_\mu + ie^2_\mu\right). \tag{4.40}$$

It is now possible to compute the components of the Weyl tensor in the null basis, as

$$\Psi_0 = C_{\mu\nu\rho\sigma}k^\mu m^\nu k^\rho m^\sigma\,, \tag{4.41a}$$

$$\Psi_1 = C_{\mu\nu\rho\sigma}k^\mu l^\nu k^\rho m^\sigma\,, \tag{4.41b}$$

$$\Psi_2 = C_{\mu\nu\rho\sigma}k^\mu m^\nu \bar{m}^\rho l^\sigma\,, \tag{4.41c}$$

$$\Psi_3 = C_{\mu\nu\rho\sigma}l^\mu k^\nu l^\rho \bar{m}^\sigma\,, \tag{4.41d}$$

$$\Psi_4 = C_{\mu\nu\rho\sigma}l^\mu \bar{m}^\nu l^\rho \bar{m}^\sigma\,, \tag{4.41e}$$

where $C_{\mu\nu\rho\sigma}$ is the Weyl tensor.

One can easily show that $\Psi_1 = \Psi_3 = 0$, while the other components are more involved. The inspection of the scalar invariants

$$I = \Psi_0\Psi_4 - 4\Psi_1\Psi_3 + 3\Psi_2^2\,, \quad J = \det\begin{pmatrix}\Psi_0 & \Psi_1 & \Psi_2\\ \Psi_1 & \Psi_2 & \Psi_3\\ \Psi_2 & \Psi_3 & \Psi_4\end{pmatrix}, \tag{4.42}$$

reveals that $I^2 \neq 27J^2$: this implies that the spacetime is algebraically general [119, 135]. Thus, the spacetime belongs to the general Petrov type I, contrary to its background (4.14) or its generating seed, which are both type D. Further, this result shows that the new black hole (4.29) does not belong to the Plebański–Demiański class of spacetimes [134].

4.3.4 Geodesics

We follow the same strategy as in the background case and define, from the metric (4.29), the following Lagrangian (dropping the inessential ω_0 term)

$$\mathscr{L} = F\left[-\left(1-\frac{2m}{r}\right)\dot{t}^2 + \frac{\dot{r}^2}{1-\frac{2m}{r}} + r^2\dot{\theta}^2\right] + F^{-1}r^2\sin^2\theta\left[\dot{\varphi} + 4\jmath(r-2m)\cos\theta\,\dot{t}\right]^2, \tag{4.43}$$

Proceeding in the same way as the background metric, we obtain the conserved charges equations and the four-momentum normalisation equations, reported in Appendix C.2.

We can extract some qualitative information, especially regarding the quantity $(r - 2m)\cos\theta$ that appears in the gravitational dragging. For stable orbits r is limited, hence the quantity $(r-2m)\cos\theta$ is limited as well. For unstable orbits we analyse the geodesic motion as r reaches infinity, thus considering large values of s. We notice that $\dot{t} \approx 0$ and $\dot{\varphi} \approx \jmath^2 L r^2 \sin^2\theta$, as $r \to \infty$, and moreover $1 - \frac{2m}{r} \approx 1$ and $F \approx \jmath^2 r^4 \sin^4\theta$. These approximations simplify the Lagrangian (4.43), that takes the form

$$\mathscr{L} \approx \jmath^2 r^4 \sin^4\theta\big(\dot{r}^2 + r^2\dot{\theta}^2\big) + \jmath^2 L^2\,. \tag{4.44}$$

The constant term is inessential and can be neglected. By changing to polar coordinates $x = r\sin\theta$ $y = r\cos\theta$, the Lagrangian boils down to

$$\mathscr{L} \approx \jmath^2 x^4\big(\dot{x}^2 + \dot{y}^2\big)\,. \tag{4.45}$$

Being the Lagrangian independent of y, we find the conserved quantity

$$A = \jmath^2 x^4 \dot{y}\,. \tag{4.46}$$

This result can be plugged into the Lagrangian, and by noticing that it does not depend explicitly on s, $d\mathscr{L}/ds = 0$, the following equation is derived:

$$\jmath^2 x^4 \dot{x}^2 + \frac{A^2}{\jmath^2 x^4} = B\,, \tag{4.47}$$

where B is a real constant. From the last equation we find

$$\dot{x} = \frac{\sqrt{B\jmath^2 x^4 - A^2}}{\jmath^2 x^4} \approx \frac{\sqrt{B}}{\jmath x^2}\,, \tag{4.48}$$

where the numerator $\sqrt{B\jmath^2 x^4 - A^2}$ depends on x which, by our change of coordinate, is proportional to r, so when r approaches infinity so does x. Therefore the constant A^2 underneath the square root can be neglected, thus justifying the approximation. Finally we get, by integration,

$$x(s) = \left(\frac{3\sqrt{B}}{\jmath}s + C\right)^{\frac{1}{3}}\,, \tag{4.49}$$

with C real constant. So $x \to \infty$ as $s \to \infty$, which means that $\dot{y} \approx 0$ and $y \approx$ constant. These results can now be plugged into the formula for the gravitational dragging, which gives

$$-\frac{g_{t\varphi}}{g_{\varphi\varphi}} = -4\jmath\left(y - 2m\frac{y}{\sqrt{x^2+y^2}}\right) \underset{s\to\infty}{\approx} -4\jmath y\,. \tag{4.50}$$

This result shows that, as $s \to \infty$, the angular velocity approaches a constant value.

We also plot the geodesic motion in spacetime (4.29): this amounts to numerically integrate the geodesic equations reported in Appendix C.2, and the results are shown in Fig. 4.4, 4.5 and C.1. More precisely, Fig. 4.4 compares geodesics in Schwarzschild

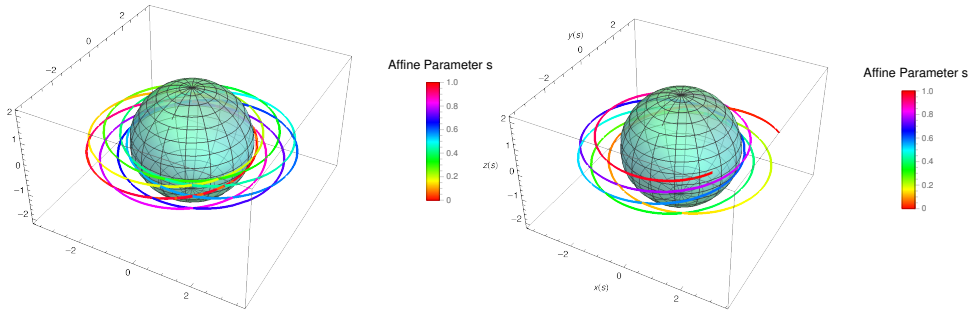

(a) $m = 1, \jmath = 0$ (b) $m = 1, \jmath = 10^{-8}$

Figure 4.4: Geodesic motion around the black hole. The left panel shows the Schwarzschild spacetime, while the right panel shows the new black hole solution (4.29). The plots share the same initial conditions with $E = 1$, $L = 12$.

spacetime (i.e. $\jmath = 0$) and geodesics in our swirling spacetime (4.29). Fig. 4.5 shows the geodesics around the black hole for different initial conditions. Finally, in Appendix C.2, Fig. C.1 pictures unstable geodesic motion for two different values of the test particle angular momentum.

4.3.5 Charges and thermodynamics

The total mass of the spacetime can be computed by means of the surface charges provided by the phase space formalism [233, 234]. We perturb the metric with respect to the parameters of the solution, and we name that variation $h_{\mu\nu} \coloneqq \delta g_{\mu\nu}$[3]. Then we find the local variation of the charge K_ξ computed along a given Killing direction ξ^μ.

The local variation of the charge must be integrated between the parametric reference background $\bar{\Psi}$ and the actual parametric configuration labelled by Ψ, on a $D-2$ dimensional surface $\mathcal{S}$ containing the event horizon $\left(d^{D-2}x\right)_{\mu\nu} = \frac{1}{2(D-2)!}\epsilon_{\mu\nu\alpha_1\dots\alpha_{D-2}}dx^{\alpha_1} \wedge \cdots \wedge dx^{\alpha_{D-2}}$. When the variation of the charge is integrable, all the parametric paths between the reference background and the solution are equivalent[4].

The result gives the total surface charge Q_ξ, defined, as in [234, 235], by

$$Q_\xi = \frac{1}{8\pi}\int_{\bar{\Psi}}^{\Psi}\int_{\mathcal{S}} K_\xi = \frac{1}{8\pi}\int_{\bar{\Psi}}^{\Psi}\int_{\mathcal{S}} K_\xi^{\mu\nu}\left(d^{D-2}x\right)_{\mu\nu}, \tag{4.51}$$

where

$$K_\xi^{\mu\nu} = \xi^\mu\nabla_\sigma h^{\nu\sigma} - \xi^\mu\nabla^\nu h - \xi_\sigma\nabla^\mu h^{\nu\sigma} - \frac{1}{2}h\nabla^\mu\xi^\nu + \frac{1}{2}h^{\sigma\mu}(\nabla_\sigma\xi^\nu - \nabla^\nu\xi_\sigma), \tag{4.52}$$

[3] In the particular case under consideration the parameter space is spanned by the mass parameter of the black hole m and by the magnitude of the rotational whirlpool dragging, $\jmath$. Thus the variation takes the form $h_{\mu\nu} = \delta g_{\mu\nu}(m,\jmath) = \partial_m g(m,\jmath)\delta m + \partial_\jmath g(m,\jmath)\delta\jmath$.

[4] In case the variation of the charge is not integrable, we still have some gauge degree of freedom in defining the frame of reference, or the normalisation of the time coordinate, to recover integrability.

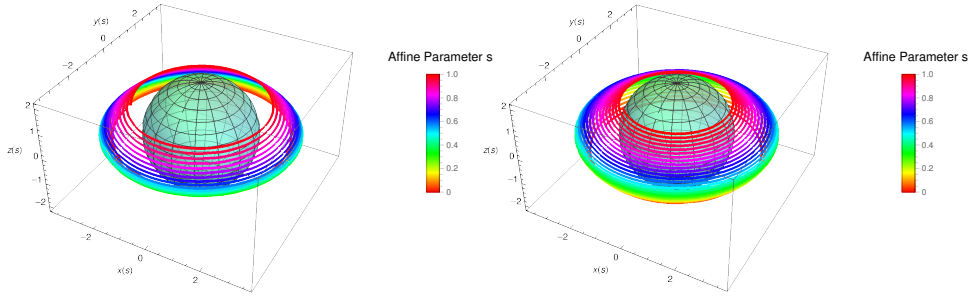

$m = 1, \jmath = 0.01$ $m = 1, \jmath = 0.01$

Figure 4.5: Embedding diagram and geodesics for the new metric (4.29) with different initial conditions, $\theta_0 = \frac{\pi}{2}$, $\dot{\theta}_0 = -\frac{1}{2}$, $L = 12$ for the l.h.s. diagram and $\theta_0 = \frac{4}{7}\pi$, $\dot{\theta}_0 = -\frac{1}{2}\sin^{-1}(\frac{4}{7}\pi)$, $L = -12$ for the r.h.s. diagram. Both representations share the following data: $E = 1$, $r_0 = 3$, $\dot{r}_0 = 1$ and $\phi_0 = \pi$.

and where $h := h^{\mu}{}_{\mu}$. If we want to compute the mass of the black hole, we have to consider the timelike Killing vector $\xi = \partial_t$, then we find

$$M = Q_{\partial_t} = m\,, \tag{4.53}$$

as for the Schwarzschild black hole. In this case the presence of the background does not modify the seed black hole mass, similarly to what happens within the context of black holes embedded in an external electromagnetic field [165]. Following this analogy we expect to observe some stronger coupling with the background in case of more general black hole seeds, as it happens in the next Section.

The angular momentum can be found analogously, just considering the Killing vector which generates the rotational symmetry ∂_φ. In this case one gets null angular momentum

$$J = Q_{\partial_\varphi} = 0\,, \tag{4.54}$$

even though the solution is clearly rotating. In fact the angular momentum refers just to the dipole term in the rotational multipolar expansion of the metric at large distances. The fact that the metric is rotating, as its non-diagonal form suggests, can be appreciated by the subsequent terms of the multipolar expansion: the quadrupole, the octupole, etc[5].

We compute the entropy and the temperature of the event horizon, in order to study the Smarr law and the thermodynamics of the black hole. The area of the even horizon is found by integrating the (θ, ϕ) part of the metric, hence

$$\mathcal{A} = \int_0^{2\pi} d\varphi \int_0^{\theta} d\theta \sqrt{g_{\theta\theta} g_{\phi\phi}}\big|_{r=2m} = 16\pi m^2\,. \tag{4.55}$$

[5]However, note that in contexts where the asymptotia is not of globally constant curvature, the notion of the gravitational multipolar expansion needs some further analysis to be clearly defined.

The entropy is given by the Bekenstein–Hawking formula $S = \mathcal{A}/4$. The validity of the area law also for this unconventional background is confirmed by the conformal field theory dual to the near-horizon geometry of the black hole. The temperature can be easily obtained via the surface gravity, $\kappa = \sqrt{-(\nabla_\mu \xi_\nu)^2/2}\big|_{r=2m}$, where $\xi = \partial_t$. We find

$$T = \frac{\kappa}{2\pi} = \frac{1}{8\pi m}\,. \tag{4.56}$$

Note that the entropy and the temperature of the black hole embedded into the swirling background are unaffected by the spacetime rotation: they remain the same of the Schwarzschild seed. Again this is peculiar of the Lie point symmetry we used to generate the solution, a general feature shared with the Harrison transformation[6].

We can easily verify the validity of the Smarr law

$$M = 2TS\,. \tag{4.57}$$

Further, the conserved charges satisfy the first law of thermodynamics

$$\delta M = T\delta S\,. \tag{4.58}$$

4.4 Kerr black hole in a swirling universe

The generating techniques discussed in Sec. 4.1 can be also exploited to embed a rotating black hole in a background endowed with its own rotation. By using the Kerr metric in Boyer–Lindquist coordinates as a seed, we obtain

$$ds^2 = F(d\varphi - \omega dt)^2 + F^{-1}\left[-\rho^2 dt^2 + \Sigma \sin^2\theta\left(\frac{dr^2}{\Delta} + d\theta^2\right)\right], \tag{4.59}$$

where the functions F^{-1} and ω can be expanded in finite power series of $\jmath$

$$F^{-1} = \chi_{(0)} + \jmath\chi_{(1)} + \jmath^2\chi_{(2)}\,, \qquad \omega = \omega_{(0)} + \jmath\omega_{(1)} + \jmath^2\omega_{(2)}\,, \tag{4.60}$$

with

$$\chi_{(0)} = \frac{R^2}{\Sigma \sin^2\theta}\,, \tag{4.61a}$$

$$\chi_{(1)} = \frac{4am\,\Xi\cos\theta}{\Sigma\sin^2\theta}\,, \tag{4.61b}$$

$$\chi_{(2)} = \frac{4a^2m^2\Xi^2\cos^2\theta + \Sigma^2\sin^4\theta}{R^2\Sigma\sin^2\theta}\,, \tag{4.61c}$$

[6]Note that this is true only when the seed does not couple with the background brought in by the transformation.

and

$$\omega_{(0)} = -\frac{2amr}{\Sigma} + \omega_0 \,, \tag{4.62a}$$

$$\omega_{(1)} = \frac{4\cos\theta[-a\Omega(r-m) + ma^4 - r^4(r-2m) - \Delta a^2 r]}{-\Sigma} \,, \tag{4.62b}$$

$$\begin{aligned}\omega_{(2)} = -\frac{2m}{\Sigma}\Big\{ & 3ar^5 - a^5(r+2m) + 2a^3r^2(r+3m) - r^3(\cos^2\theta - 6)\Omega \\ & + a^2[\cos^2\theta(3r-2m) - 6(r-m)]\Omega\Big\} \,,\end{aligned} \tag{4.62c}$$

where

$$\Delta = r^2 - 2mr + a^2 \,, \qquad \rho^2 = \Delta\sin^2\theta \,, \tag{4.63a}$$

$$\Sigma = (r^2+a^2)^2 - \Delta a^2\sin^2\theta \,, \qquad \Omega = \Delta a\cos^2\theta \,, \tag{4.63b}$$

$$\Xi = r^2(\cos^2\theta - 3) - a^2(1+\cos^2\theta) \,, \qquad R^2 = r^2 + a^2\cos^2\theta \,. \tag{4.63c}$$

When $\jmath = 0$ we recover the seed metric, i.e. the Kerr black hole. For $\jmath \neq 0$ we have the direct generalisation of the metric (4.12).

However we notice that in this case, because of the spin-spin interaction between the black hole and the background frame dragging, an extra force acts on the axis of symmetry. But since it is not symmetric on the two hemispheres, the metric is affected by non-removable conical singularities, indeed

$$\lim_{\theta\to 0}\frac{1}{\theta}\int_0^{2\pi}\sqrt{\frac{g_{\varphi\varphi}}{g_{\theta\theta}}}d\varphi = \frac{2\pi}{(1-4am\jmath)^2} \neq \lim_{\theta\to\pi}\frac{1}{\pi-\theta}\int_0^{2\pi}\sqrt{\frac{g_{\varphi\varphi}}{g_{\theta\theta}}}d\varphi = \frac{2\pi}{(1+4am\jmath)^2} \,. \tag{4.64}$$

In fact, even though the background spinning parameter $\jmath$ couples to the Kerr angular momentum (for unit of mass) a, it is not possible to find a relation among the physical parameters to remove simultaneously both angular defects, unless of course for known subcases such as Kerr, for $\jmath = 0$, the spacetime discussed in Sec. 4.3 for $a = 0$, or the rotating background for $m = 0$. The presence of a non-removable conical singularity implies that a cosmic string or a strut (with their δ-like stress-energy-momentum tensor on a portion of the z-axis) have to be postulated in order to compensate the "force" effect induced by the spin-spin interaction of the black hole with the background, which would tent to add acceleration to the black hole[7].

In the case one wants to immerse the Kerr–Newman black hole into this spinning universe, one has to use the charged generalised version of the Ehlers transformation, as described in Chapter 1.

[7]The metric considered in this Section does not posses the acceleration parameter: one should work with the rotating C-metric to consistently include the acceleration. That is why, in this Section, the role of the string uniquely results in the effect of compensating the spin coupling.

4.5 Double-Wick rotation of the background: flat Taub–NUT spacetime

Given the analogies between the rotating background (4.16) and the Melvin spacetime, and given that the analytical continuation of the Melvin universe corresponds to the Reissner–Nordström metric with a flat base manifold, it is natural to inquire about an analog analytical continuation for the rotating background. At this scope, we implement a double Wick rotation between time and the azimuthal angle $t \to i\phi$, $\varphi \to i\tau$ of the metric (4.16). Redefining the integration constant of the rotating background as $\jmath = m/2\ell^3$, changing the coordinate $\rho = \ell\sqrt{2r/m}$ and after the rescaling of the other three coordinates we obtain

$$ds^2 = -\frac{2mr}{r^2+\ell^2}(dt - 2\ell\theta d\phi)^2 + \frac{r^2+\ell^2}{2mr}dr^2 + (r^2+\ell^2)(d\theta^2 + d\phi^2)\,. \tag{4.65}$$

It is not hard to recognise the Taub–NUT spacetime with a flat, or possibly cylindrical if we keep the azimuthal angle identification, base manifold. In fact, the flat Taub–NUT metric can be generated via the Ehlers transformation[8] from the Schwarzschild metric, previously composed with a double-Wick rotation[9]. Note that the Ehlers transformation can be used to build, from the Minkowski seed, the rotating background, just considering $m = 0$ in the procedure of Sec. 4.1. This is analogous to what happens to the Melvin universe, which can be obtained from Minkowski spacetime via the Harrison transformation and whose double-Wick dual corresponds to the flat Reissner–Nordström metric. This fact strengthens the link between the Melvin universe and our rotating background. Actually this correspondence can be summarized by the following proportion:

$$\text{Melvin Universe : Harrison transformation = Rotating Universe : Ehlers transformation} \tag{4.66}$$

This formal analogy can be exploited to build new solutions, even outside the range of the generating technique based on the Lie point symmetries of the Ernst equations: that is important because the symmetry transformations such as the Ehlers and the Harrison maps break in the presence of the cosmological constant. However, as noted in [132], the Melvin universe can still be generalised when the cosmological constant is not zero, and it still preserves its relation with the flat Reissner–Nordström metric with a constant curvature base manifold[10]. Therefore, thanks to the analogy with the Melvin case, we have in our hand a procedure to generalise the rotating background (4.16) in the presence of the cosmological constant.

It is sufficient to operate a double-Wick rotation of the cosmological version of the

[8] In this Section we are referring to transformations applied to the *magnetic* LWP metric, as explained in Sec. 4.1.

[9] While this is true for a generic sign of the constant curvature of the seed base manifold, only the metric with positive curvature can be interpreted as a black hole in Einstein gravity.

[10] Metrics without a topological spherical base manifold are interpreted as black holes only in the presence of the cosmological constant.

flat Taub–NUT metric (4.65)

$$\begin{aligned} ds^2 = &-\frac{\frac{\Lambda}{3}r^4 + 2\ell^2\Lambda r^2 + 2mr - \ell^4\Lambda}{r^2+\ell^2}(dt - 2\ell\theta d\phi)^2 \\ &+ \frac{(r^2+\ell^2)}{\frac{\Lambda}{3}r^4 + 2\ell^2\Lambda r^2 + 2mr - \ell^4\Lambda}dr^2 + (r^2+\ell^2)(d\theta^2 + d\phi^2)\,. \end{aligned} \tag{4.67}$$

Thus, using the same change of coordinates and parametrisation of the case above, we get

$$\begin{aligned} ds^2 = (1+\jmath^2\rho^4)&\left(-d\tau^2 + \frac{\rho^2}{\frac{\Lambda}{4\jmath^2} + \rho^2 - \frac{\Lambda}{2}\rho^4 - \frac{\jmath^2\Lambda}{12}\rho^8}d\rho^2 + dz^2\right) \\ &+ \left(\frac{\Lambda}{4\jmath^2} + \rho^2 - \frac{\Lambda}{2}\rho^4 - \frac{\jmath^2\Lambda}{12}\rho^8\right)\frac{(d\psi + 4\jmath z d\tau)^2}{1+\jmath^2\rho^4}\,. \end{aligned} \tag{4.68}$$

It is not difficult to realise that this metric still corresponds, up to a change of coordinates, to the non-expanding and non-accelerating Kuntdt class of the Plebański–Demiański family presented in Eq. (16.26) of [135]. The explicit change of coordinates works as in Sec. 4.2, namely $q = 2\jmath z$ and $p^2 = \rho$, together with the rescaling $t \to \jmath t$ and the redefinitions $\gamma = 1/\jmath$, $\tilde{\Lambda} = 4\Lambda$. Then, metric (4.68) becomes

$$ds^2 = (\gamma^2 + p^2)\left(-d\tau^2 + \frac{dp^2}{\mathcal{P}} + dq^2\right) + \frac{\mathcal{P}}{\gamma^2+p^2}(d\psi + 2\gamma q d\tau)^2\,, \tag{4.69}$$

where

$$\mathcal{P} = \gamma^4\tilde{\Lambda} + \gamma^2 p - 2\gamma^2\tilde{\Lambda}p^2 - \frac{\tilde{\Lambda}}{3}p^4\,. \tag{4.70}$$

The latter corresponds to Eq. (16.26) of [135], where $m = e = g = \alpha = \epsilon_2 = 0$, $\epsilon_0 = 1$, $k = \gamma^4\tilde{\Lambda}$, $\epsilon = 2\gamma^2\tilde{\Lambda}$ and $n = \gamma^2/2$.

The analogy between the rotating background and the Taub–NUT spacetime can be pushed further: it is known [217] that the Melvin spacetime corresponds to a couple of magnetically charged Reissner–Nordström black holes moved towards infinity. In this sense, the magnetic field which permeates the Melvin spacetime is nothing but the field generated by two black hole sources at infinity. Thus, it is natural to ask ourselves if a similar construction also holds for the rotating background (4.14), i.e. if it can be obtained as a limit of a double black hole metric.

By relying on the above considerations and, more specifically, on the proportion (4.66), the natural candidate for an "ancestor" metric is the double-Taub–NUT spacetime with opposite NUT parameters [26]: the rotation of the two counter-rotating Taub–NUT black holes, once they are pushed at infinity, should produce the rotation of the background that is experienced in the background spacetime. This interpretation is also consistent with the behaviour of the angular velocity (4.32): we noticed that the angular velocity increases in opposite directions in the two hemisphere, coherently with the fact that the two black holes rotate in different directions. Moreover this picture is enforced by the geometry of the ergoregions, since the latter thrive for large values of z on the axis of symmetry.

4.6 Outlook

The transformation we studied in this Chapter, which consists in a proper composition of the Ehlers transformation with a discrete symmetry, allows us to take advantage of the Ernst solution generating technique to non-linearly superpose the Schwarzschild black hole and a swirling universe. The background geometry can be interpreted as a gravitational whirlpool generated by a couple of counter-rotating sources at infinity. Its frame dragging transforms the static Schwarzschild metric into a stationary one, removing the asymptotic flatness, but without drastically altering the black hole causal structure nor introducing pathological features. The analogies between the swirling background and the Melvin universe are numerous, like the metric structure, the ergoregions and the deformations engraved on the event horizon: in fact the former universe can be considered as the rotating counterpart of the latter.

For this reason we expect that this spinning background can be used as a regularising instrument for metric with conical singularities, exactly as the electromagnetic background brought by the Harrison transformation does. In the former case to have non-trivial physical effects one needs to exploit the interplay between the coupling of the electromagnetic field of the seed with the one of the background, as suggested by the analysis of the transformed Kerr metric, in Sec. 4.4. Indeed the interaction between the Kerr parameter a and the background parameter $\jmath$ generates an additional "force" which impels the system to accelerate. Unfortunately, the geometry of the spacetime is not general enough to accommodate this physical feature into that metric, yielding a conical singularity which compensates the mutual rotational coupling. On the other hand we count that the spin-spin interaction between the seed and the background environment can play a relevant role into the regularisation of gravitational models which otherwise would be mathematically defective and physically incomplete. For instance, in the same way as Ernst showed that the electromagnetic background can remove the conical defect of the accelerating and charged black hole, we foresee that the procedure presented in this paper can remove the axial singularities of the rotating C-metric, providing at the same time a reasonable physical explication for its acceleration [236]. Also this model furnishes alternative scenarios for black hole nucleation and pair creation, without relying on the electromagnetic field, as discussed in the literature so far [187, 188, 185].

Clearly this procedure may be relevant for other systems, not necessarily accelerating, such as balancing multi-black hole sources to reach an equilibrium configuration. Also in that case the frame dragging of the background can play a role in removing cosmic strings or strut from the singular spacetime. On the other hand, preliminary studies suggest that the spin-spin interaction between the swirling universe and a Taub–NUT spacetime are not sufficient to mend also the singular behaviour of that metric, i.e. to remove the Misner string[11].

[11] Obviously we are referring to the non-compact time representation of the Taub–NUT metric, because when one considers proper periodic identification of the temporal coordinate the spacetime can be regularised. Unfortunately, the latter interpretation violates causality because of the appearance of closed timelike curves,

From a phenomenological point of view our rotating background might be of some interest in the description of black holes surrounded by interacting matter, which produces intense frame dragging, such as the one caused by the collision of counter-rotating galaxies.

Since this construction is based on a symmetry transformation of the Ernst equations, it can be directly generalised to the Einstein–Maxwell case, to the minimally and conformally coupled scalar field case and, more generally, to scalar-tensor theories such as Brans–Dicke, just by using the adequate Ehlers transformation as described in Sec. 1.1 and in [237] respectively. The embedding method presented here may reveal useful in estabilishing and improving traversability of wormhole spacetimes.

which makes this picture nonphysical.

Conclusions

Black holes represent one of the most fascinating areas of research in contemporary physics: they are bizarre objects that challenge our common sense, and whose existence represented a mystery for many years. They are also the natural candidate for studying quantum gravity, as the region close to a curvature singularity is characterised by strong gravity on very small scales. As explained in the Introduction, binary and, more generally, multi-black hole systems are relevant for the experiments and for the structure of the gravitational theories. Thus, it is important to find regular multi-source solutions that can describe actual astrophysical black holes and, from the theoretical point of view, to properly define the thermodynamics of such systems: indeed, the thermodynamics can give important hints about the microscopic origin of the entropy and the temperature.

In this Thesis, we have studied some configurations that allow one to regularise multi-black hole spacetimes, with the aid of solution generating techniques.

We began by introducing such techniques and explaining the details of their functioning in Chapter 1, which provided us with the machinery necessary to the construction of our solutions. We also reported an historical perspective on the development of the various solution generating methods over the years, commenting on the peculiar features and on the pros and cons of the different approaches.

Then, in Chapter 2, we introduced an external gravitational field as a regularising background, and discussed its properties and multipolar character. We provided many examples of singularity-free multi-black hole spacetimes: static, rotating, charged an accelerating systems of black holes were studied and analysed in detail. They share the common feature of being regularised by an appropriate tuning of the external field parameters, i.e. by choosing the multipole coefficients in order to balance the attraction among the black holes. We inspected the action of the external field on the geometry of these "deformed" black holes, and we verified that the thermodynamics of these objects was well defined: this allowed us to conclude that these multi-black hole systems are physically well posed. Moreover, the external fields have a phenomenological interest since they can model matter surrounding black holes.

Chapter 3 introduced the bubbles of nothing to the business of the multi-black hole regularisation: the bubbles, which are usually studied in relation to the vacuum stability, were considered as time-dependent expanding spacetimes that can win against the mutual collapse of many black holes. We showed that bubbles of nothing have a deep connection with black holes, as it can be appreciated by taking some appropriate limits which bring a bubble into a black hole, and viceversa (an analog construction works for bubbles in five dimensions and black rings). Further, we embedded multi-black holes (in four dimensions) and black rings (in five dimensions) in bubble spacetimes, and explicitly showed that they reach an equilibrium configuration. We also considered other examples that involve accelerating black holes (in four dimensions) and black Saturn and di-ring (in five dimensions), and how the manipulation of their rod diagrams naturally allows one to move from one configuration to another. Thus, bubbles revealed to be very powerful solutions, which permit to obtain solutions free of conical singularities, and moreover we proved that their connection to elementary black hole solutions in General Relativity is deeper than one may expect.

Finally, in Chapter 4 we introduced a transformation that add a "swirling" background to a given spacetime. Such a rotational character acts as a sort of whirlpool, which drags the observers that are at rest in the spacetime, as shown by the embedding diagrams of the geodesics. A static black hole embedded in the swirling geometry is (perhaps surprisingly) not affected by conical singularities: it is possible to properly define conserved charges and thermodynamics, and to study ergoregions and geometrical properties. On the other hand, the swirling rotation couples to the angular momentum of a black hole, as shown by the Kerr solution: in that case, conical singularities appear and the solution is no more regular. This drawback, however, paves the way to a possible mechanism to regularise a multi-black hole spacetime: the embedding of a double-Kerr solution into the swirling background and the resulting coupling between the swirl parameter and the spin-spin interaction of the holes, might provide a mechanism to remove the conical singularities. This is a very promising idea, that can be pursued in a future research.

Appendices

APPENDIX A

Conical singularities and energy conditions

Conical singularities, beyond making the spacetime manifold ill-defined from a mathematical point of view, give also rise to energy issues. In general, such singularities can be interpreted as strings or struts whose energy-momentum tensor has a δ-like nature. We show what are the physical issues that the conical singularities bring in when they are present in the spacetime.

Let us consider Minkowski spacetime with an wedge of angle $2\pi\alpha\prime$ artificially removed. By defining $C = 1 - \alpha\prime$, we can write the metric as

$$ds^2 = -dt^2 + dr^2 + C^2 r^2 d\varphi^2 + dz^2 \,, \tag{A.1}$$

where $0 \leq \varphi < 2\pi$. One can regard this spacetime as a field sourced by a cosmic string or a strut [238], whose non-vanishing energy-momentum tensor components are

$$T_t^t = T_\varphi^\varphi = 2\pi\mu\,\delta(x,y)\,, \tag{A.2}$$

where

$$\mu = \frac{1-C}{4C}\,, \tag{A.3}$$

and $\delta(x,y)$ is the two-dimensional delta function depending on the coordinates orthogonal to the z-axis (x,y). μ is interpreted as the tension of the filament source.

This result can be generalised to a generic four-dimensional spacetime [239], for which one finds that the Einstein equations $G_{\mu\nu} = 8\pi T_{\mu\nu}$ give rise to an energy-momentum tensor

$$T_0^0 = T_3^3 = 2\pi\mu\,\delta(x,y)\,, \tag{A.4}$$

where now

$$\mu = \frac{2\pi - C}{4C}\,. \tag{A.5}$$

C represents again the angular excess/deficit for the azimuthal angle.

Let us consider, e.g., a two-black hole spacetime from (2.18) ($N = 2$): the result (A.4) clearly shows that for $\mu > 0$ (positive tension), the source acts as a string that pull a black hole. This is the behaviour of the conical singularities that one finds at $z < w_1$ and $z > w_4$ There are no negative-energy issues in this case, but the string extends to infinity and the δ function gives rise to a divergent energy-momentum tensor.

In the case of $\mu < 0$ (negative tension), the conical singularity in $w_2 < z < w_3$ acts as a strut which pushes apart the two black holes. The energy density associated to the energy-momentum tensor is negative (i.e. the strut is composed of anti-gravitational matter) and there is again a divergence due to the δ function.

APPENDIX B

Harrison and Kramer–Neugebauer charging trasformations

Both the Harrison and the Kramer–Neugebauer [173] transformations are two symmetries of the Ernst equations for the Einstein–Maxwell theory presented in Chapter 1. As it was explained there, the complex Ernst equations enjoy an $SU(2,1)$ Lie-point symmetry group spanned by the finite transformations (1.46)

The Harrison transformation is given by Eq. (1.46e), while the Kramer–Neugebauer one, as defined in [240] to charge the Kerr metric embedded in an external gravitational field, is

$$\mathcal{E}' = \frac{\mathcal{E} - \zeta^2}{1 - \zeta^2 \mathcal{E}}\,, \qquad \Phi' = \frac{\zeta(\mathcal{E} - 1)}{1 - \zeta^2 \mathcal{E}}\,. \tag{B.1}$$

The latter transformation reduces to the one in (2.63) for static and uncharged seeds. Since both the Kramer–Neugebauer transformation (B.1) and the Harrison transformation (1.46e) have the same physical effects (they add an electric monopole to an uncharged seed), we have the suspect that they are basically the same transformation, up to gauge transformations. In fact it can be shown that the subsequent composition of transformations (1.46a), (1.46d) and (1.46e) to an Ernst seed $(\mathcal{E}, \Phi)$ gives

$$\mathcal{E}' = \frac{\lambda\lambda^*\mathcal{E} - \beta^*(\beta + 2\lambda\Phi)}{1 + \alpha^2(-2\beta + \alpha^*\beta\beta^* - \alpha\lambda\lambda^*\mathcal{E} + 2\lambda(\alpha\beta^* - 1)\Phi}\,, \tag{B.2}$$

$$\Phi' = \frac{\beta - \alpha\beta\beta^* + \lambda\lambda^*\alpha\mathcal{E} + \Phi - 2\lambda\alpha\beta^*\Phi}{1 + \alpha^2(-2\beta + \alpha^*\beta\beta^* - \alpha\lambda\lambda^*\mathcal{E} + 2\lambda(\alpha\beta^* - 1)\Phi}\,. \tag{B.3}$$

Then considering a null electromagnetic Ernst potential, $\Phi = 0$, the imaginary part of the parameters α, β, λ equal to zero and choosing

$$\lambda = \frac{1}{1 - \zeta^2}\,, \qquad \alpha = \zeta\,, \qquad \beta = -\frac{\zeta}{1 - \zeta^2}\,, \tag{B.4}$$

we exactly recover the transformation (B.1). In case of static metrics the latter further simplifies to Eqs. (2.63). Therefore the Kramer–Neugebauer and the Harrison transfomration are basically equivalent, up to gauge transformations, so they might be called collectively Harrison–Kramer–Neugebauer transformation.

As an explicit example we show the efficacy of the charging transformation (2.63) on an asymptotically flat, static and discharged metric: acting on the Schwarzschild metric, we are able to produce the Reissner–Nordström black hole.

For simplicity we take the seed in spherical symmetric coordinates

$$ds^2 = -\left(1 - \frac{2m}{r}\right)dt^2 + \frac{dr^2}{1 - \frac{2m}{r}} + r^2 d\theta^2 + r^2 \sin^2\theta d\varphi^2 \,, \tag{B.5}$$

from which we can easily read

$$e^{2\psi} = 1 - \frac{2m}{r} \,, \qquad A_t = 0 \,. \tag{B.6}$$

After the charging transformation (2.63) we get the new solution

$$e^{2\hat{\psi}} = \frac{r(r-2m)(1-\zeta^2)^2}{[r + (2m-r)\zeta^2]^2} \,, \quad \hat{A}_t = -\frac{2m\zeta}{r + (2m-r)\zeta^2} \,. \tag{B.7}$$

A shift of the radial coordinate

$$r \to \hat{r} - M + \sqrt{M^2 - q^2} \,, \tag{B.8}$$

and a rescaling of the parameters

$$\zeta \to \frac{M - \sqrt{M^2 - q^2}}{q} \,, \qquad m \to \sqrt{M^2 - q^2} \,, \tag{B.9}$$

suffice to recognise the standard Reissner–Norström spacetime

$$d\hat{s}^2 = -\left(1 - \frac{2M}{\hat{r}} + \frac{q^2}{\hat{r}^2}\right)dt^2 + \frac{d\hat{r}^2}{1 - \frac{2M}{\hat{r}} + \frac{q^2}{\hat{r}^2}} + \hat{r}^2 d\theta^2 + \hat{r}^2 \sin^2\theta d\varphi^2 \,, \tag{B.10}$$

$$\hat{A} = -\frac{q}{\hat{r}}\, dt \,. \tag{B.11}$$

APPENDIX C

Geodesics of the swirling spacetime

We report here the explicit expression for the geodesic equation from Chapter 4, both for the background and the full black hole metric.

C.1 Background geodesics

The explicit expressions for the definitions of the conserved quantities (4.23) are

$$\dot{t} = \frac{E + 4\jmath Lz}{1 + \jmath^2\rho^4}\,, \qquad \dot{\phi} = \jmath^2 L\rho^2 + \frac{L}{\rho^2} - 4\jmath z\frac{E + 4\jmath Lz}{1 + \jmath^2\rho^4}\,. \tag{C.1}$$

By substituting these relations into the Lagrangian (4.22), we get

$$\mathscr{L} = (1 + \jmath^2\rho^2)\left[\frac{L^2}{\rho^2} - \left(\frac{E + 4\jmath Lz}{1 + \jmath^2\rho^4}\right)^2 + \dot{\rho}^2 + \dot{z}^2\right]. \tag{C.2}$$

The equation coming from the normalisation of the four-momentum $u_\mu u^\mu = \chi$ is

$$\begin{aligned}\dot{\rho}^2 + \dot{z}^2 = \frac{1}{(1 + \jmath^2\rho^4)^2}\Bigg[&E^2 - 8\jmath Lz(E + 6\jmath Lz) + \frac{L^2}{\rho^2} + 2\jmath^2 L^2\rho^2 + \jmath^4 L^2\rho^6 \\ &+ \left(4\sqrt{2}\jmath\rho z\frac{E + 4\jmath Lz}{1 + \jmath^2\rho^4}\right)^2\Bigg] + \frac{\chi}{1 + \jmath^2\rho^4}\,.\end{aligned} \tag{C.3}$$

C.2 Black hole geodesics

The conserved charges equations are

$$\dot{t} = \frac{r[E + 4\jmath L\cos\theta(r - 2m)]}{(r - 2m)(1 + \jmath^2 r^4\sin^4\theta)}\,, \tag{C.1a}$$

$$\dot{\phi} = \frac{L - \jmath r^3\sin^2\theta[4\cos\theta(E - 8\jmath Lm\cos\theta) - \jmath^3 Lr^5\sin^6\theta + 2\jmath Lr(9\cos^2\theta - 1)]}{r^2\sin^2\theta(1 + \jmath^2 r^4\sin^4\theta)}\,. \tag{C.1b}$$

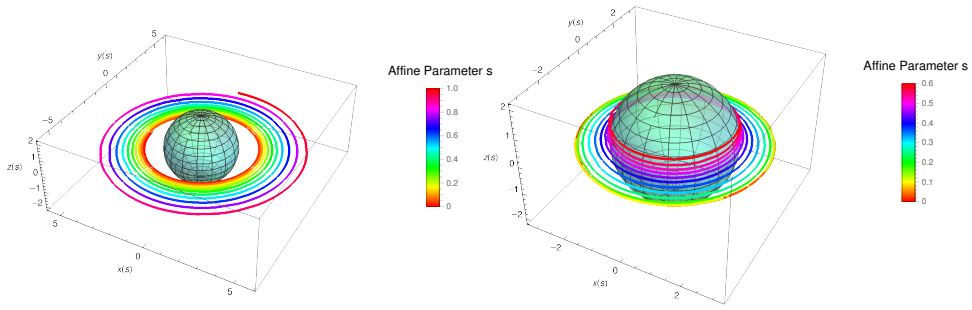

(a) $m = 1, \jmath = 0.01, L = 1$ (b) $m = 1, \jmath = 0.01, L = 36$

Figure C.1: Black hole (4.29) with two different unstable orbits. The first one represents the case where L is small and shows that the orbit approaches an asymptotic value. The second one shows an orbit with large L: the test particle on the plane defined by $\theta = \pi/2$ is attracted towards the black hole.

L is the angular momentum and E is the energy. From the conservation of the four-momentum it follows

$$\begin{aligned}\left(1+\jmath^2 r^4 \sin^4\theta\right)\left[\left(\frac{r(E+4\jmath L\cos\theta(r-2m))}{(r-2m)(1+\jmath^2 r^4\sin^4\theta)}\right)^2+\frac{\dot r^2}{1-\frac{2m}{r}}+r^2\dot\theta^2\right]\\ +\frac{L^2(1+\jmath^2 r^4\sin^4\theta)^2}{r^4\sin^4\theta}=\chi\,.\end{aligned} \tag{C.2}$$

APPENDIX D

Zipoy–Voorhees spacetime embedded in the swirling universe

We apply the procedure described in Sec. 4.1 to a slightly more general metric than the Schwarzschild black hole, the Zipoy–Voorhees metric [138, 241, 242]. This class of spacetime is relevant in General Relativity because, thanks to its rich multipolar expansion, can be used to model the exterior gravitational field of planets or stars. It is worth to mention, in connection with Chapter 2, that Kerns and Wild constructed a version of the Zipoy–Voorhees spacetime embedded in the external gravitational field [243].

The Zipoy–Voorhees metric can be of some interest, when supported by a conformally coupled scalar field, to build hairy black holes or wormholes such as the Bekenstein black hole [74] or the Barcelo–Visser wormhole [76][1]. In particular, the presence of the swirling background might be useful in the wormhole configuration to improve both the stability and the traversability properties of the solution.

We start by casting the Zipoy–Voorhees seed in terms of the magnetic LWP metric (1.48) in prolate spherical coordinates

$$d\bar{s}^2 = \bar{f}\big(d\phi - \bar{\omega}d\tau\big)^2 + \frac{1}{\bar{f}}\left[-\rho^2 d\tau^2 + \kappa^2(x^2-y^2)e^{2\bar{\gamma}}\left(\frac{dx^2}{x^2-1}+\frac{dy^2}{1-y^2}\right)\right], \tag{D.1}$$

where

$$\bar{f}(x,y) = \kappa^2\left(\frac{x-1}{x+1}\right)^{-\delta}(x^2-1)(1-y^2)\,, \tag{D.2a}$$

$$\bar{\gamma}(x,y) = \frac{1}{2}\log\left[\kappa^2\left(\frac{x-1}{x+1}\right)^{-2\delta}(x^2-1)(1-y^2)\left(\frac{x^2-1}{x^2-y^2}\right)^{\delta^2}\right], \tag{D.2b}$$

$$\rho(x,y) = \kappa\sqrt{(x^2-1)(y^2-1)}\,. \tag{D.2c}$$

Clearly, this metric reduces to the static Schwarzschild black hole of Sec. 4.1 when $\delta = 1$. For generic values of $\delta \neq 1$, the metric looses the spherical symmetry and presents naked singularities outside the event horizon, hence it is not suitable for describing legit black

[1] Actually the associated complex Ernst field equations remain the same of the pure general relativistic case, so as the main structure functions in the metric. Only the decoupled function γ has to be slightly modified according to [75].

holes in pure General Relativity. However, for $\delta = 1/2$, when properly coupled with a scalar field, it represents the first hairy black hole ever discovered [74].

Thanks to the Ehlers transformation (4.2), and following the same procedure illustrated in Sec. 4.1, we are able to embed the Zipoy–Vorhees metric into the swirling background. The $\bar{\gamma}$ function remains the same, while

$$f(x,y) = \frac{\kappa^2(1-y^2)(x^2-1)^{1+\delta}}{(x-1)^{2\delta} + \jmath^2(1+x)^{2\delta}(x^2-1)^2(1-y^2)^2}\,, \tag{D.3a}$$

$$\omega(x,y) = 4\jmath\kappa^2 y(x-\delta) + \omega_0\,. \tag{D.3b}$$

The metric defined by (D.1) and (D.3) represents the δ extension of the spacetime (4.12), therefore the Zipoy–Voorhees spacetime immersed in the rotating background described in Sec. 4.2. Further generalisations with angular momentum can be built straightforwardly, starting with seeds of the family of the Tomimatsu–Sato solutions [244, 245].

Bibliography

[1] A. Einstein. Zur Allgemeinen Relativitätstheorie. *Sitzungsber. Preuss. Akad. Wiss. Berlin (Math. Phys.)*, 1915:778–786, 1915. [Addendum: Sitzungsber.Preuss.Akad.Wiss.Berlin (Math.Phys.) 1915, 799–801 (1915)].

[2] D. Hilbert. Die Grundlagen der Physik. 1. *Gott. Nachr.*, 27:395–407, 1915.

[3] F.W. Dyson, A.S. Eddington, and C. Davidson. A Determination of the Deflection of Light by the Sun's Gravitational Field, from Observations Made at the Total Eclipse of May 29, 1919. *Phil. Trans. Roy. Soc. Lond. A*, 220:291–333, 1920. doi:10.1098/rsta.1920.0009.

[4] B. Bertotti, L. Iess, and P. Tortora. A test of general relativity using radio links with the Cassini spacecraft. *Nature*, 425:374–376, 2003. doi:10.1038/nature01997.

[5] T.E. Collett, L.J. Oldham, R.J. Smith, M.W. Auger, K.B. Westfall, D. Bacon, R.C. Nichol, K.L. Masters, K. Koyama, and R. van den Bosch. A precise extragalactic test of General Relativity. *Science*, 360:1342, 2018. arXiv:1806.08300, doi:10.1126/science.aao2469.

[6] B.P. Abbott et al. Observation of Gravitational Waves from a Binary Black Hole Merger. *Phys. Rev. Lett.*, 116(6):061102, 2016. arXiv:1602.03837, doi:10.1103/PhysRevLett.116.061102.

[7] C.M. Will. The Confrontation between General Relativity and Experiment. *Living Rev. Rel.*, 17:4, 2014. arXiv:1403.7377, doi:10.12942/lrr-2014-4.

[8] K. Schwarzschild. On the gravitational field of a mass point according to Einstein's theory. *Sitzungsber. Preuss. Akad. Wiss. Berlin (Math. Phys.)*, 1916:189–196, 1916. arXiv:physics/9905030.

[9] M. Parsa, A. Eckart, B. Shahzamanian, V. Karas, M. Zajaček, J.A. Zensus, and C. Straubmeier. Investigating the relativistic motion of the stars near the supermassive black hole in the galactic center. *The Astrophysical Journal*, 845(1):22, aug 2017. doi:10.3847/1538-4357/aa7bf0.

[10] A. Boehle, A.M. Ghez, R. Schödel, L. Meyer, S. Yelda, S. Albers, G.D. Martinez, E.E. Becklin, T. Do, J.R. Lu, K. Matthews, M.R. Morris, B. Sitarski, and G. Witzel. An improved distance and mass estimate for sgr a* from a multistar orbit analysis. *The Astrophysical Journal*, 830(1):17, oct 2016. doi:10.3847/0004-637x/830/1/17.

[11] The GRAVITY Collaboration. A geometric distance measurement to the galactic center black hole with 0.3% uncertainty. *A&A*, 625:L10, 2019. doi:10.1051/0004-6361/201935656.

[12] K. Akiyama et al. First M87 Event Horizon Telescope Results. I. The Shadow of the Supermassive Black Hole. *Astrophys. J. Lett.*, 875:L1, 2019. arXiv:1906.11238, doi:10.3847/2041-8213/ab0ec7.

[13] K. Akiyama et al. First M87 Event Horizon Telescope Results. II. Array and Instrumentation. *Astrophys. J. Lett.*, 875(1):L2, 2019. arXiv:1906.11239, doi:10.3847/2041-8213/ab0c96.

[14] K. Akiyama et al. First M87 Event Horizon Telescope Results. III. Data Processing and Calibration. *Astrophys. J. Lett.*, 875(1):L3, 2019. arXiv:1906.11240, doi:10.3847/2041-8213/ab0c57.

[15] K. Akiyama et al. First M87 Event Horizon Telescope Results. IV. Imaging the Central Supermassive Black Hole. *Astrophys. J. Lett.*, 875(1):L4, 2019. arXiv:1906.11241, doi:10.3847/2041-8213/ab0e85.

[16] K. Akiyama et al. First M87 Event Horizon Telescope Results. V. Physical Origin of the Asymmetric Ring. *Astrophys. J. Lett.*, 875(1):L5, 2019. arXiv:1906.11242, doi:10.3847/2041-8213/ab0f43.

[17] K. Akiyama et al. First M87 Event Horizon Telescope Results. VI. The Shadow and Mass of the Central Black Hole. *Astrophys. J. Lett.*, 875(1):L6, 2019. arXiv:1906.11243, doi:10.3847/2041-8213/ab1141.

[18] R.P. Kerr. Gravitational field of a spinning mass as an example of algebraically special metrics. *Phys. Rev. Lett.*, 11:237–238, 1963. doi:10.1103/PhysRevLett.11.237.

[19] S. Hod. Late time evolution of realistic rotating collapse and the no hair theorem. *Phys. Rev. D*, 58:104022, 1998. arXiv:gr-qc/9811032, doi:10.1103/PhysRevD.58.104022.

[20] B.P. Abbott et al. GW151226: Observation of Gravitational Waves from a 22-Solar-Mass Binary Black Hole Coalescence. *Phys. Rev. Lett.*, 116(24):241103, 2016. arXiv:1606.04855, doi:10.1103/PhysRevLett.116.241103.

[21] B.P. Abbott et al. GW170104: Observation of a 50-Solar-Mass Binary Black Hole Coalescence at Redshift 0.2. *Phys. Rev. Lett.*, 118(22):221101, 2017. [Erratum: Phys.Rev.Lett. 121, 129901 (2018)]. arXiv:1706.01812, doi:10.1103/PhysRevLett.118.221101.

[22] B.P. Abbott et al. GWTC-1: A Gravitational-Wave Transient Catalog of Compact Binary Mergers Observed by LIGO and Virgo during the First and Second Observing Runs. *Phys. Rev. X*, 9(3):031040, 2019. arXiv:1811.12907, doi:10.1103/PhysRevX.9.031040.

[23] B.P. Abbott et al. GW170817: Observation of Gravitational Waves from a Binary Neutron Star Inspiral. *Phys. Rev. Lett.*, 119(16):161101, 2017. arXiv:1710.05832, doi:10.1103/PhysRevLett.119.161101.

[24] B.P. Abbott et al. Gravitational Waves and Gamma-rays from a Binary Neutron Star Merger: GW170817 and GRB 170817A. *Astrophys. J. Lett.*, 848(2):L13, 2017. arXiv:1710.05834, doi:10.3847/2041-8213/aa920c.

[25] J. Hennig. On the balance problem for two rotating and charged black holes. *Class. Quant. Grav.*, 36(23):235001, 2019. arXiv:1906.04847, doi:10.1088/1361-6382/ab4f41.

[26] D. Kramer and G. Neugebauer. The superposition of two kerr solutions. *Physics Letters A*, 75(4):259 – 261, 1980.

[27] G. Neugebauer. A general integral of the axially symmetric stationary einstein equations. *Journal of Physics A: Mathematical and General*, 13(2):L19–L21, feb 1980. doi:10.1088/0305-4470/13/2/003.

[28] P.T. Chrusciel, M. Eckstein, L. Nguyen, and S.J. Szybka. Existence of singularities in two-Kerr black holes. *Class. Quant. Grav.*, 28:245017, 2011. arXiv:1111.1448, doi:10.1088/0264-9381/28/24/245017.

[29] G. Neugebauer and J. Hennig. Non-existence of stationary two-black-hole configurations. *Gen. Rel. Grav.*, 41:2113–2130, 2009. arXiv:0905.4179, doi:10.1007/s10714-009-0840-8.

[30] J. Hennig and G. Neugebauer. Non-existence of stationary two-black-hole configurations: The degenerate case. *Gen. Rel. Grav.*, 43:3139–3162, 2011. arXiv:1103.5248, doi:10.1007/s10714-011-1228-0.

[31] G. Neugebauer and J. Hennig. Stationary two-black-hole configurations: A non-existence proof. *J. Geom. Phys.*, 62:613–630, 2012. arXiv:1105.5830, doi:10.1016/j.geomphys.2011.05.008.

[32] V.S. Manko and E. Ruiz. Metric for two arbitrary Kerr sources. *Phys. Lett. B*, 794:36–40, 2019. arXiv:1806.10408, doi:10.1016/j.physletb.2019.05.027.

[33] J. Hennig, C. Cederbaum, and M. Ansorg. A Universal inequality for axisymmetric and stationary black holes with surrounding matter in the Einstein-Maxwell theory. *Commun. Math. Phys.*, 293:449–467, 2010. arXiv:0812.2811, doi:10.1007/s00220-009-0889-y.

[34] A. Papapetrou. A static solution of the equations of the gravitational field for an arbitary charge-distribution. *Proceedings of the Royal Irish Academy. Section A: Mathematical and Physical Sciences*, 51:191–204, 1945. URL: http://www.jstor.org/stable/20488481.

[35] S.D. Majumdar. A class of exact solutions of Einstein's field equations. *Phys. Rev.*, 72:390–398, 1947. doi:10.1103/PhysRev.72.390.

[36] D. Kastor and J.H. Traschen. Cosmological multi - black hole solutions. *Phys. Rev. D*, 47:5370–5375, 1993. arXiv:hep-th/9212035, doi:10.1103/PhysRevD.47.5370.

[37] S. Chimento and D. Klemm. Multicentered black holes with a negative cosmological constant. *Phys. Rev. D*, 89(2):024037, 2014. arXiv:1311.6937, doi:10.1103/PhysRevD.89.024037.

[38] K.S. Thorne. Disk accretion onto a black hole. 2. Evolution of the hole. *Astrophys. J.*, 191:507–520, 1974. doi:10.1086/152991.

[39] P.T. Chrusciel and P. Tod. The Classification of static electro-vacuum spacetimes containing an asymptotically flat spacelike hypersurface with compact interior. *Commun. Math. Phys.*, 271:577–589, 2007. arXiv:gr-qc/0512043, doi:10.1007/s00220-007-0191-9.

[40] G.A. Alekseev and V.A. Belinski. Superposition of fields of two rotating charged masses in general relativity and existence of equilibrium configurations. *Gen. Rel. Grav.*, 51(5):68, 2019. arXiv:1905.05317, doi:10.1007/s10714-019-2543-0.

[41] I. Cabrera-Munguia. Metric for two unequal extreme Kerr-Newman black holes. *Phys. Lett. B*, 826:136895, 2022. arXiv:2110.04879, doi:10.1016/j.physletb.2022.136895.

[42] G.A. Alekseev. Thirty years of studies of integrable reductions of Einstein's field equations. In *12th Marcel Grossmann Meeting on General Relativity*, pages 645–666, 11 2010. arXiv:1011.3846, doi:10.1142/9789814374552_0033.

[43] C.S. Gardner, J.M. Greene, M.D. Kruskal, and R.M. Miura. Method for solving the Korteweg-deVries equation. *Phys. Rev. Lett.*, 19:1095–1097, 1967. doi:10.1103/PhysRevLett.19.1095.

[44] F.J. Ernst. New formulation of the axially symmetric gravitational field problem. *Phys. Rev.*, 167:1175–1179, 1968. doi:10.1103/PhysRev.167.1175.

[45] F.J. Ernst. New formulation of the axially symmetric gravitational field problem. ii. *Phys. Rev.*, 168:1415–1417, Apr 1968. doi:10.1103/PhysRev.168.1415.

[46] R.P. Geroch. A Method for generating new solutions of Einstein's equation. 2. *J. Math. Phys.*, 13:394–404, 1972. doi:10.1063/1.1665990.

[47] W. Kinnersley. Symmetries of the Stationary Einstein-Maxwell Field Equations. 1. *J. Math. Phys.*, 18:1529–1537, 1977. doi:10.1063/1.523458.

[48] W. Kinnersley and D.M. Chitre. Symmetries of the Stationary Einstein-Maxwell Field Equations. 2. *J. Math. Phys.*, 18:1538–1542, 1977. doi:10.1063/1.523459.

[49] W. Kinnersley and D.M. Chitre. Symmetries of the Stationary Einstein-Maxwell Field Equations. 3. *J. Math. Phys.*, 19:1926–1931, 1978. doi:10.1063/1.523912.

[50] W. Kinnersley and D.M. Chitre. Symmetries of the stationary Einstein–Maxwell equations. IV. Transformations which preserve asymptotic flatness. *J. Math. Phys.*, 19:2037–2042, 1978. doi:10.1063/1.523580.

[51] D. Maison. Are the stationary, axially symmetric Einstein equations completely integrable? *Phys. Rev. Lett.*, 41:521, 1978. doi:10.1103/PhysRevLett.41.521.

[52] V.A. Belinsky and V.E. Zakharov. Integration of the Einstein Equations by the Inverse Scattering Problem Technique and the Calculation of the Exact Soliton Solutions. *Sov. Phys. JETP*, 48:985–994, 1978.

[53] V.A. Belinsky and V.E. Sakharov. Stationary Gravitational Solitons with Axial Symmetry. *Sov. Phys. JETP*, 50:1–9, 1979.

[54] G.A. Alekseev. N-soliton solutions of einstein-maxwell equations. *JETP Lett. (Engl. Transl.); (United States)*, 32:4, 8 1980. URL: https://www.osti.gov/biblio/6803745.

[55] B.K. Harrison. Bäcklund transformation for the ernst equation of general relativity. *Phys. Rev. Lett.*, 41:1197–1200, Oct 1978. URL: https://link.aps.org/doi/10.1103/PhysRevLett.41.1197, doi:10.1103/PhysRevLett.41.1197.

[56] F.B. Estabrook and H.D. Wahlquist. Prolongation Structures of Nonlinear Evolution Equations. 2. *J. Math. Phys.*, 17:1293–1297, 1976. doi:10.1063/1.523056.

[57] G. Neugebauer. Backlund transformations of axially symmetric stationary gravitational fields. *J. Phys. A*, 12:L67–L70, 1979. doi:10.1088/0305-4470/12/4/001.

[58] G. Neugebauer. Recursive calculation of axially symmetric stationary einstein fields. *Journal of Physics A: Mathematical and General*, 13(5):1737–1740, may 1980. doi:10.1088/0305-4470/13/5/031.

[59] B. Julia. Kac-Moody symmetry of gravitation and supergravity theories. In *American Mathematical Society summer seminar on Appication of Group Theory in Physics and Mathematical Physics*, 9 1982.

[60] B. Julia. Application of sueprgravity to gravitation theory. In *International School of Cosmology and Gravitation: 8th Course: Unified Field Theories of More than Four Dimensions, Including Exact Solutions*, 8 1982.

[61] P. Breitenlohner and D. Maison. On the Geroch Group. *Ann. Inst. H. Poincare Phys. Theor.*, 46:215, 1987.

[62] I. Hauser and F.J. Ernst. Integral equation method for effecting Kinnersley-Chitre transformations. *Phys. Rev. D*, 20:362–369, 1979. doi:10.1103/PhysRevD.20.362.

[63] I. Hauser and F.J. Ernst. Integral equation method for effecting Kinnersley-Chitre transformations. II. *Phys. Rev. D*, 20:1783–1790, 1979. doi:10.1103/PhysRevD.20.1783.

[64] I. Hauser and F.J. Ernst. A homogeneous Hilbert problem for the Kinnersley–Chitre transformations. *Journal of Mathematical Physics*, 21(5):1126–1140, 1980. doi:10.1063/1.524536.

[65] I. Hauser and F.J. Ernst. A homogeneous hilbert problem for the kinnersley–chitre transformations of electrovac space-times. *Journal of Mathematical Physics*, 21(6):1418–1422, 1980.

[66] I. Hauser and F.J. Ernst. Proof of a geroch conjecture. *Journal of Mathematical Physics*, 22(5):1051–1063, 1981. doi:10.1063/1.525012.

[67] N.R. Sibgatullin. Construction of the general solution of the system of einstein–maxwell equations for the stationary axisymmetric case. In *Soviet Physics-Doklady*, volume 29, pages 802–804, 1984.

[68] N.R. Sibgatullin. *Oscillations and waves in strong gravitational and electromagnetic fields*. Springer-Verlag, 1991.

[69] G.A. Alekseev. The Method of the Inverse Problem of Scattering and the Singular Integral Equations for Interacting Massless Fields. *Sov. Phys. Dokl.*, 30:565–568, 1985.

[70] G.A. Alekseev. Exact solutions in the general theory of relativity. *Trudy Matematicheskogo Instituta imeni VA Steklova*, 176:211–258, 1987.

[71] G.A. Alekseev. Isomonodromy deformations and integrability of electrovacuum einstein-maxwell field equations with isometries. In *Solitons and applications (Dubna, 1989)*, pages 174–179. World Sci. Publ., River Edge, NJ, 1990.

[72] G.A. Alekseev. Monodromy transform approach to solution of the Ernst equations in general relativity. In *International European Conference on Gravitation: Journees Relativistes 99*, 9 1999. arXiv:gr-qc/9912109.

[73] V.A. Belinsky. One soliton cosmological waves. *Sov. Phys. JETP*, 50:623–631, 1979.

[74] J.D. Bekenstein. Black Holes with Scalar Charge. *Annals Phys.*, 91:75–82, 1975. doi:10.1016/0003-4916(75)90279-1.

[75] M. Astorino. Stationary axisymmetric spacetimes with a conformally coupled scalar field. *Phys. Rev. D*, 91:064066, 2015. arXiv:1412.3539, doi:10.1103/PhysRevD.91.064066.

[76] C. Barcelo and M. Visser. Traversable wormholes from massless conformally coupled scalar fields. *Phys. Lett. B*, 466:127–134, 1999. arXiv:gr-qc/9908029, doi:10.1016/S0370-2693(99)01117-X.

[77] D.V. Galtsov, A.A. Garcia, and O.V. Kechkin. Symmetries of the stationary Einstein-Maxwell dilaton theory. *Class. Quant. Grav.*, 12:2887–2903, 1995. arXiv:hep-th/9504155, doi:10.1088/0264-9381/12/12/007.

[78] D.V. Galtsov and A. A. Garcia. Hidden symmetries in dilaton gravity. *Phys. Rev. D*, 52:3432–3439, 1995. doi:10.1103/PhysRevD.52.3432.

[79] D.V. Galtsov and O.V. Kechkin. Ehlers-Harrison type transformations in dilaton - axion gravity. *Phys. Rev. D*, 50:7394–7399, 1994. arXiv:hep-th/9407155, doi:10.1103/PhysRevD.50.7394.

[80] A. Garcia, D. Galtsov, and O. Kechkin. Class of stationary axisymmetric solutions of the Einstein-Maxwell dilaton - axion field equations. *Phys. Rev. Lett.*, 74:1276–1279, 1995. doi:10.1103/PhysRevLett.74.1276.

[81] D.V. Gal'tsov and P.S. Letelier. Ehlers-Harrison transformations and black holes in dilaton - axion gravity with multiple vector fields. *Phys. Rev. D*, 55:3580–3592, 1997. arXiv:gr-qc/9612007, doi:10.1103/PhysRevD.55.3580.

[82] D.V. Gal'tsov and S.A. Sharakin. Matrix Ernst potentials for EMDA with multiple vector fields. *Phys. Lett. B*, 399:250–257, 1997. arXiv:hep-th/9702039, doi:10.1016/S0370-2693(97)00295-5.

[83] A.A. Pomeransky. Complete integrability of higher-dimensional Einstein equations with additional symmetry, and rotating black holes. *Phys. Rev. D*, 73:044004, 2006. arXiv:hep-th/0507250, doi:10.1103/PhysRevD.73.044004.

[84] A.A. Pomeransky and R.A. Sen'kov. Black ring with two angular momenta, 12 2006. arXiv:hep-th/0612005.

[85] R.C. Myers and M.J. Perry. Black Holes in Higher Dimensional Space-Times. *Annals Phys.*, 172:304, 1986. doi:10.1016/0003-4916(86)90186-7.

[86] R. Emparan and H.S. Reall. A Rotating black ring solution in five-dimensions. *Phys. Rev. Lett.*, 88:101101, 2002. arXiv:hep-th/0110260, doi:10.1103/PhysRevLett.88.101101.

[87] H. Iguchi and T. Mishima. Solitonic generation of five-dimensional black ring solution. *Phys. Rev. D*, 73:121501, 2006. arXiv:hep-th/0604050, doi:10.1103/PhysRevD.73.121501.

[88] S. Tomizawa, Y. Morisawa, and Y. Yasui. Vacuum solutions of five dimensional Einstein equations generated by inverse scattering method. *Phys. Rev. D*, 73:064009, 2006. arXiv:hep-th/0512252, doi:10.1103/PhysRevD.73.064009.

[89] S. Tomizawa and M. Nozawa. Vacuum solutions of five-dimensional Einstein equations generated by inverse scattering method. II. Production of black ring solution. *Phys. Rev. D*, 73:124034, 2006. arXiv:hep-th/0604067, doi:10.1103/PhysRevD.73.124034.

[90] T. Mishima and H. Iguchi. New axisymmetric stationary solutions of five-dimensional vacuum Einstein equations with asymptotic flatness. *Phys. Rev. D*, 73:044030, 2006. arXiv:hep-th/0504018, doi:10.1103/PhysRevD.73.044030.

[91] Y. Chen and E. Teo. Rotating black rings on Taub-NUT. *JHEP*, 06:068, 2012. arXiv:1204.3116, doi:10.1007/JHEP06(2012)068.

[92] H. Iguchi, K. Izumi, and T. Mishima. Systematic solution-generation of five-dimensional black holes. *Prog. Theor. Phys. Suppl.*, 189:93–125, 2011. arXiv:1106.0387, doi:10.1143/PTPS.189.93.

[93] H. Elvang and P. Figueras. Black Saturn. *JHEP*, 05:050, 2007. arXiv:hep-th/0701035, doi:10.1088/1126-6708/2007/05/050.

[94] H. Iguchi and T. Mishima. Black di-ring and infinite nonuniqueness. *Phys. Rev. D*, 75:064018, 2007. [Erratum: Phys.Rev.D 78, 069903 (2008)]. arXiv:hep-th/0701043, doi:10.1103/PhysRevD.78.069903.

[95] J. Evslin and C. Krishnan. The Black Di-Ring: An Inverse Scattering Construction. *Class. Quant. Grav.*, 26:125018, 2009. arXiv:0706.1231, doi:10.1088/0264-9381/26/12/125018.

[96] H. Elvang and M.J. Rodriguez. Bicycling Black Rings. *JHEP*, 04:045, 2008. arXiv:0712.2425, doi:10.1088/1126-6708/2008/04/045.

[97] J.V. Rocha, M.J. Rodriguez, and A. Virmani. Inverse Scattering Construction of a Dipole Black Ring. *JHEP*, 11:008, 2011. arXiv:1108.3527, doi:10.1007/JHEP11(2011)008.

[98] R. Emparan and H.S. Reall. Black Rings. *Class. Quant. Grav.*, 23:R169, 2006. arXiv:hep-th/0608012, doi:10.1088/0264-9381/23/20/R01.

[99] R. Emparan and H.S. Reall. Black Holes in Higher Dimensions. *Living Rev. Rel.*, 11:6, 2008. arXiv:0801.3471, doi:10.12942/lrr-2008-6.

[100] S.S. Yazadjiev. Completely integrable sector in 5-D Einstein-Maxwell gravity and derivation of the dipole black ring solutions. *Phys. Rev. D*, 73:104007, 2006. arXiv:hep-th/0602116, doi:10.1103/PhysRevD.73.104007.

[101] I. Bakas. Solitons of axion - dilaton gravity. *Phys. Rev. D*, 54:6424–6434, 1996. arXiv:hep-th/9605043, doi:10.1103/PhysRevD.54.6424.

[102] I. Bakas. 2-D gravisolitons in string theory. In *2nd International Sakharov Conference on Physics*, pages 350–354, 6 1996. arXiv:hep-th/9606030.

[103] A. Bouchareb, G. Clement, C.-M. Chen, D.V. Gal'tsov, N.G. Scherbluk, and T. Wolf. G(2) generating technique for minimal D=5 supergravity and black rings. *Phys. Rev. D*, 76:104032, 2007. [Erratum: Phys.Rev.D 78, 029901 (2008)]. arXiv:0708.2361, doi:10.1103/PhysRevD.76.104032.

[104] D.V. Gal'tsov and N.G. Scherbluk. Hidden symmetries in 5D supergravities and black rings. *PoS*, BHGRS:016, 2008. arXiv:0912.2770, doi:10.22323/1.075.0016.

[105] D.V. Gal'tsov and N.G. Scherbluk. Generating technique for U(1)**3 5D supergravity. *Phys. Rev. D*, 78:064033, 2008. arXiv:0805.3924, doi:10.1103/PhysRevD.78.064033.

[106] D.V. Gal'tsov and N.G. Scherbluk. Improved generating technique for D=5 supergravities and squashed Kaluza-Klein Black Holes. *Phys. Rev. D*, 79:064020, 2009. arXiv:0812.2336, doi:10.1103/PhysRevD.79.064020.

[107] P. Figueras, E. Jamsin, J.V. Rocha, and A. Virmani. Integrability of Five Dimensional Minimal Supergravity and Charged Rotating Black Holes. *Class. Quant. Grav.*, 27:135011, 2010. arXiv:0912.3199, doi:10.1088/0264-9381/27/13/135011.

[108] D. Katsimpouri, A. Kleinschmidt, and A. Virmani. Inverse Scattering and the Geroch Group. *JHEP*, 02:011, 2013. arXiv:1211.3044, doi:10.1007/JHEP02(2013)011.

[109] D. Katsimpouri, A. Kleinschmidt, and A. Virmani. An inverse scattering formalism for STU supergravity. *JHEP*, 03:101, 2014. arXiv:1311.7018, doi:10.1007/JHEP03(2014)101.

[110] D. Katsimpouri, A. Kleinschmidt, and A. Virmani. An Inverse Scattering Construction of the JMaRT Fuzzball. *JHEP*, 12:070, 2014. arXiv:1409.6471, doi:10.1007/JHEP12(2014)070.

[111] G.A. Alekseev. Integrability of generalized (matrix) Ernst equations in string theory. *Theor. Math. Phys.*, 144:1065–1074, 2005. arXiv:hep-th/0410246, doi:10.1007/s11232-005-0136-4.

[112] G.A. Alekseev. Integrability of the symmetry reduced bosonic dynamics and soliton generating transformations in the low energy heterotic string effective theory. *Phys. Rev. D*, 80:041901, 2009. arXiv:0811.1358, doi:10.1103/PhysRevD.80.041901.

[113] M. Godazgar and H.S. Reall. Algebraically special axisymmetric solutions of the higher-dimensional vacuum Einstein equation. *Class. Quant. Grav.*, 26:165009, 2009. arXiv:0904.4368, doi:10.1088/0264-9381/26/16/165009.

[114] J. Ehlers. Konstruktionen und Charakterisierung von Losungen der Einsteinschen Gravitationsfeldgleichungen. Phd thesis, Hamburg University, 1957.

[115] B.K. Harrison. New solutions of the einstein-maxwell equations from old. *Journal of Mathematical Physics*, 9(11):1744–1752, 1968. doi:10.1063/1.1664508.

[116] C. Reina and A. Treves. Nut-like generalization of axisymmetric gravitational fields. *Journal of Mathematical Physics*, 16(4):834–835, 1975. doi:10.1063/1.522614.

[117] F.J. Ernst. Black holes in a magnetic universe. *J. Math. Phys.*, 17(1):54–56, 1976. doi:10.1063/1.522781.

[118] M. Heusler. *Black Hole Uniqueness Theorems*. Cambridge Lecture Notes in Physics. Cambridge University Press, 1996. doi:10.1017/CBO9780511661396.

[119] H. Stephani, D. Kramer, M.A.H. MacCallum, C. Hoenselaers, and E. Herlt. *Exact solutions of Einstein's field equations*. Cambridge Monographs on Mathematical Physics. Cambridge Univ. Press, Cambridge, 2003. doi:10.1017/CBO9780511535185.

[120] H. Stephani. *Differential Equations: Their Solution Using Symmetries*. Cambridge University Press, 1990. doi:10.1017/CBO9780511599941.

[121] R. Martelli. The Action of the Axisymmetric and Stationary Symmetry Group of General Relativity on a Static Black Hole. Bachelor thesis, Milan U., 2022.

[122] G. Neugebauer and D. Kramer. Eine methode zur konstruktion stationärer einstein-maxwell-felder. *Annalen der Physik*, 479(1-2):62–71, 1969. doi:https://doi.org/10.1002/andp.19694790108.

[123] W. Kinnersley. Generation of stationary einstein-maxwell fields. *Journal of Mathematical Physics*, 14(5):651–653, 1973. doi:10.1063/1.1666373.

[124] A.H. Taub. Empty space-times admitting a three parameter group of motions. *Annals Math.*, 53:472–490, 1951. doi:10.2307/1969567.

[125] E. Newman, L. Tamburino, and T. Unti. Empty space generalization of the Schwarzschild metric. *J. Math. Phys.*, 4:915, 1963. doi:10.1063/1.1704018.

[126] C.W. Misner. Taub-Nut Space as a counterexample to almost anything. In J. Ehlers, editor, *Relativity Theory and Astrophysics. Vol.1: Relativity and Cosmology*, volume 8, page 160. Rhode Island: American Mathematical Society, 1967.

[127] G. Clément, D. Gal'tsov, and M. Guenouche. Rehabilitating space-times with NUTs. *Phys. Lett. B*, 750:591–594, 2015. arXiv:1508.07622, doi:10.1016/j.physletb.2015.09.074.

[128] H. Reissner. Über die eigengravitation des elektrischen feldes nach der einsteinschen theorie. *Annalen der Physik*, 355(9):106–120, 1916. doi:https://doi.org/10.1002/andp.19163550905.

[129] G. Nordström. On the Energy of the Gravitation field in Einstein's Theory. *Koninklijke Nederlandse Akademie van Wetenschappen Proceedings Series B Physical Sciences*, 20:1238–1245, January 1918.

[130] M.A. Melvin. Pure magnetic and electric geons. *Phys. Lett.*, 8:65–70, 1964. doi:10.1016/0031-9163(64)90801-7.

[131] G.W. Gibbons and D.L. Wiltshire. Space-Time as a Membrane in Higher Dimensions. *Nucl. Phys. B*, 287:717–742, 1987. arXiv:hep-th/0109093, doi:10.1016/0550-3213(87)90125-8.

[132] M. Astorino. Charging axisymmetric space-times with cosmological constant. *JHEP*, 06:086, 2012. arXiv:1205.6998, doi:10.1007/JHEP06(2012)086.

[133] V. Belinski and E. Verdaguer. *Gravitational solitons*. Cambridge Monographs on Mathematical Physics. Cambridge University Press, 2005. doi:10.1017/CBO9780511535253.

[134] J.F. Plebanski and M. Demianski. Rotating, charged, and uniformly accelerating mass in general relativity. *Annals Phys.*, 98:98–127, 1976. doi:10.1016/0003-4916(76)90240-2.

[135] J.B. Griffiths and J. Podolsky. *Exact Space-Times in Einstein's General Relativity*. Cambridge Monographs on Mathematical Physics. Cambridge University Press, Cambridge, 2009. doi:10.1017/CBO9780511635397.

[136] K. Hong and E. Teo. A New form of the rotating C-metric. *Class. Quant. Grav.*, 22:109–118, 2005. arXiv:gr-qc/0410002, doi:10.1088/0264-9381/22/1/007.

[137] T. Harmark. Stationary and axisymmetric solutions of higher-dimensional general relativity. *Phys. Rev. D*, 70:124002, 2004. URL: 10.1103/PhysRevD.70.124002, arXiv:hep-th/0408141, doi:10.1103/PhysRevD.70.124002.

[138] R. Bach and H. Weyl. Neue lösungen der einsteinschen gravitationsgleichungen. *Mathematische Zeitschrift*, 13(1):134–145, 1922.

[139] W. Israel and K.A. Khan. Collinear particles and bondi dipoles in general relativity. *Il Nuovo Cimento*, 33(2):331–344, 1964. doi:https://doi.org/10.1007/BF02750196.

[140] P.S. Letelier and S.R. de Oliveira. Double Kerr-NUT space-times: Spinning strings and spinning rods. *Phys. Lett. A*, 238:101–106, 1998. doi:10.1016/S0375-9601(97)00730-5.

[141] G. Erez and N. Rosen. The gravitational field of a particle possessing a multipole moment. *Bull. Research Council Israel*, Sect. F.8, 9 1959.

[142] G.M. de Castro and P.S. Letelier. Black holes surrounded by thin rings and the stability of circular orbits. *Class. Quant. Grav.*, 28:225020, 2011. doi:10.1088/0264-9381/28/22/225020.

[143] R. Beig and R.M. Schoen. On static n-body configurations in relativity. *Classical and Quantum Gravity*, 26(7):075014, mar 2009. doi:10.1088/0264-9381/26/7/075014.

[144] A.G. Doroshkevich, Y.B. Zel'dovich, and I.D. Novikov. Gravitational Collapse of Non-Symmetric and Rotating Bodies. *Zhurnal Eksperimentalnoi i Teoreticheskoi Fiziki*, 49:170, December 1965.

[145] S. Chandrasekhar. *The mathematical theory of black holes*. Clarendon Press, Oxford, 1985.

[146] R.P. Geroch and J.B. Hartle. Distorted black holes. *J. Math. Phys.*, 23:680, 1982. doi:10.1063/1.525384.

[147] F.J. Ernst. Generalized c-metric. *Journal of Mathematical Physics*, 19(9):1986–1987, 1978. doi:https://doi.org/10.1063/1.523896.

[148] R.M. Kerns and W.J. Wild. Black hole in a gravitational field. *General Relativity and Gravitation*, 14(1):1–4, 1982.

[149] M. Astorino and A. Viganò. Binary black hole system at equilibrium. *Phys. Lett. B*, 820:136506, 2021. arXiv:2104.07686, doi:10.1016/j.physletb.2021.136506.

[150] M. Astorino and A. Viganò. Charged and rotating multi-black holes in an external gravitational field. *Eur. Phys. J. C*, 82(9):829, 2022. arXiv:2105.02894, doi:10.1140/epjc/s10052-022-10787-y.

[151] M. Astorino and A. Viganò. Many accelerating distorted black holes. *Eur. Phys. J. C*, 81(10):891, 2021. arXiv:2106.02058, doi:10.1140/epjc/s10052-021-09693-6.

[152] N. Breton, A.A. Garcia, V. S. Manko, and T.E. Denisova. Arbitrarily deformed Kerr Newman black hole in an external gravitational field. *Phys. Rev. D*, 57:3382–3388, 1998. doi:10.1103/PhysRevD.57.3382.

[153] W. Israel. Event horizons in static vacuum space-times. *Phys. Rev.*, 164:1776–1779, 1967. doi:10.1103/PhysRev.164.1776.

[154] S. Abdolrahimi, J. Kunz, P. Nedkova, and C. Tzounis. Properties of the distorted Kerr black hole. *JCAP*, 12:009, 2015. arXiv:1509.01665, doi:10.1088/1475-7516/2015/12/009.

[155] R.P. Geroch. Multipole moments. II. Curved space. *J. Math. Phys.*, 11:2580–2588, 1970. doi:10.1063/1.1665427.

[156] R. O. Hansen. Multipole moments of stationary space-times. *J. Math. Phys.*, 15:46–52, 1974. doi:10.1063/1.1666501.

[157] G. Fodor, C. Hoenselaers, and Z. Perjés. Multipole moments of axisymmetric systems in relativity. *Journal of Mathematical Physics*, 30(10):2252–2257, 1989. doi:10.1063/1.528551.

[158] P.S. Letelier. Multipole stationary soliton solutions to the einstein equations. *Revista Brasileira de Fisica*, 14:371–376, September 1984.

[159] R.C. Myers. Higher Dimensional Black Holes in Compactified Space-times. *Phys. Rev. D*, 35:455, 1987. doi:10.1103/PhysRevD.35.455.

[160] R. Gregory, Z.L. Lim, and A. Scoins. Thermodynamics of Many Black Holes. *Front. in Phys.*, 9:187, 2021. arXiv:2012.15561, doi:10.3389/fphy.2021.666041.

[161] A. Komar. Covariant conservation laws in general relativity. *Phys. Rev.*, 113:934–936, Feb 1959. doi:10.1103/PhysRev.113.934.

[162] A. Tomimatsu. Equilibrium of Two Rotating Charged Black Holes and the Dirac String. *Prog. Theor. Phys.*, 72:73, 1984. doi:10.1143/PTP.72.73.

[163] M. Henneaux and C. Teitelboim. Asymptotically anti-De Sitter Spaces. *Commun. Math. Phys.*, 98:391–424, 1985. doi:10.1007/BF01205790.

[164] A. Ashtekar, S. Fairhurst, and B. Krishnan. Isolated horizons: Hamiltonian evolution and the first law. *Phys. Rev. D*, 62:104025, 2000. arXiv:gr-qc/0005083, doi:10.1103/PhysRevD.62.104025.

[165] M. Astorino, G. Compère, R. Oliveri, and N. Vandevoorde. Mass of Kerr-Newman black holes in an external magnetic field. *Phys. Rev. D*, 94(2):024019, 2016. arXiv:1602.08110, doi:10.1103/PhysRevD.94.024019.

[166] J.B. Hartle and S.W. Hawking. Path Integral Derivation of Black Hole Radiance. *Phys. Rev. D*, 13:2188–2203, 1976. doi:10.1103/PhysRevD.13.2188.

[167] L. Smarr. Mass formula for Kerr black holes. *Phys. Rev. Lett.*, 30:71–73, 1973. [Erratum: Phys.Rev.Lett. 30, 521–521 (1973)]. doi:10.1103/PhysRevLett.30.71.

[168] D. Christodoulou and R. Ruffini. Reversible transformations of a charged black hole. *Phys. Rev. D*, 4:3552–3555, 1971. doi:10.1103/PhysRevD.4.3552.

[169] M.M. Caldarelli, G. Cognola, and D. Klemm. Thermodynamics of Kerr-Newman-AdS black holes and conformal field theories. *Class. Quant. Grav.*, 17:399–420, 2000. arXiv:hep-th/9908022, doi:10.1088/0264-9381/17/2/310.

[170] M. Astorino. Thermodynamics of Regular Accelerating Black Holes. *Phys. Rev. D*, 95(6):064007, 2017. arXiv:1612.04387, doi:10.1103/PhysRevD.95.064007.

[171] A. Tomimatsu. Distorted rotating black holes. *Physics Letters A*, 103(8):374–376, 1984. URL: https://www.sciencedirect.com/science/article/pii/0375960184901348, doi:https://doi.org/10.1016/0375-9601(84)90134-8.

[172] M. Astorino. Enhanced Ehlers Transformation and the Majumdar-Papapetrou-NUT Spacetime. *JHEP*, 01:123, 2020. arXiv:1906.08228, doi:10.1007/JHEP01(2020)123.

[173] D. Kramer and G. Neugebauer. Eine exakte stationäre lösung der einstein-maxwell-gleichungen. *Annalen der Physik*, 479(1-2):59–61, 1969. doi:https://doi.org/10.1002/andp.19694790107.

[174] G.A. Alekseev and V.A. Belinski. Equilibrium configurations of two charged masses in General Relativity. *Phys. Rev. D*, 76:021501, 2007. arXiv:0706.1981, doi:10.1103/PhysRevD.76.021501.

[175] V.S. Manko. The Double-Reissner-Nordstrom solution and the interaction force between two spherically symmetric charged particles. *Phys. Rev. D*, 76:124032, 2007. arXiv:0710.2158, doi:10.1103/PhysRevD.76.124032.

[176] R. Emparan and E. Teo. Macroscopic and microscopic description of black diholes. *Nucl. Phys. B*, 610:190–214, 2001. arXiv:hep-th/0104206, doi:10.1016/S0550-3213(01)00319-4.

[177] V.S. Manko and N.R. Sibgatullin. Construction of exact solutions of the Einstein-Maxwell equations corresponding to a given behaviour of the Ernst potentials on the symmetry axis. *Classical and Quantum Gravity*, 10(7):1383–1404, July 1993. doi:10.1088/0264-9381/10/7/014.

[178] C.A.R. Herdeiro and C. Rebelo. On the interaction between two Kerr black holes. *JHEP*, 10:017, 2008. arXiv:0808.3941, doi:10.1088/1126-6708/2008/10/017.

[179] G.W. Gibbons. The Motion of black holes. *Commun. Math. Phys.*, 35:13–23, 1974. doi:10.1007/BF01646451.

[180] H.F. Dowker and S.N. Thambyahpillai. Many accelerating black holes. *Class. Quant. Grav.*, 20:127–136, 2003. arXiv:gr-qc/0105044, doi:10.1088/0264-9381/20/1/310.

[181] P.S. Letelier. Static and stationary multiple soliton solutions to the einstein equations. *Journal of Mathematical Physics*, 26(3):467–476, 1985. doi:10.1063/1.526633.

[182] J.B. Griffiths, P. Krtous, and J. Podolsky. Interpreting the C-metric. *Class. Quant. Grav.*, 23:6745–6766, 2006. arXiv:gr-qc/0609056, doi:10.1088/0264-9381/23/23/008.

[183] K. Hong and E. Teo. A New form of the C metric. *Class. Quant. Grav.*, 20:3269–3277, 2003. arXiv:gr-qc/0305089, doi:10.1088/0264-9381/20/14/321.

[184] W.B. Bonnor. An exact solution of einstein's equations for two particles falling freely in an external gravitational field. *General relativity and gravitation*, 20(6):607–622, 1988. doi:https://doi.org/10.1007/BF00758917.

[185] M. Astorino. Pair Creation of Rotating Black Holes. *Phys. Rev. D*, 89(4):044022, 2014. arXiv:1312.1723, doi:10.1103/PhysRevD.89.044022.

[186] G.W. Gibbons. Quantized flux tubes in Einstein-Maxwell theory and noncompact internal spaces. In *22nd Winter School of Theoretical Physics: Fields and Geometry*, 5 1986.

[187] D. Garfinkle, S.B. Giddings, and A. Strominger. Entropy in black hole pair production. *Phys. Rev. D*, 49:958–965, 1994. arXiv:gr-qc/9306023, doi:10.1103/PhysRevD.49.958.

[188] S.W. Hawking, G.T. Horowitz, and S.F. Ross. Entropy, Area, and black hole pairs. *Phys. Rev. D*, 51:4302–4314, 1995. arXiv:gr-qc/9409013, doi:10.1103/PhysRevD.51.4302.

[189] W.B. Bonnor. Static magnetic fields in general relativity. *Proceedings of the Physical Society. Section A*, 67(3):225, 1954. doi:https://doi.org/10.1088/0370-1298/67/3/305.

[190] H.E.J. Curzon. Cylindrical solutions of einstein's gravitation equations. *Proceedings of the London Mathematical Society*, 2(1):477–480, 1925. doi:https://doi.org/10.1112/plms/s2-23.1.477.

[191] J. Chazy. Sur le champ de gravitation de deux masses fixes dans la théorie de la relativité. *Bulletin de la Societe mathematique de France*, 52:17–38, 1924. doi:https://doi.org/10.24033/bsmf.1044.

[192] A. Einstein and N. Rosen. Two-Body Problem in General Relativity Theory. *Phys. Rev.*, 49:404–405, 1936. doi:10.1103/PhysRev.49.404.2.

[193] W.B. Bonnor and N.S. Swaminarayan. An exact solution for uniformly accelerated particles in general relativity. *Zeitschrift für Physik*, 177(3):240–256, 1964. doi:https://doi.org/10.1007/BF01375497.

[194] J. Bicak, C. Hoenselaers, and B.G. Schmidt. The solutions of the einstein equations for uniformly accelerated particles without nodal singularities. i. freely falling particles in external fields. *Proceedings of the Royal Society of London. A. Mathematical and Physical Sciences*, 390(1799):397–409, 1983. doi:10.1098/rspa.1983.0138.

[195] J. Bicak and V. Pravda. Spinning C metric: Radiative space-time with accelerating, rotating black holes. *Phys. Rev. D*, 60:044004, 1999. arXiv:gr-qc/9902075, doi:10.1103/PhysRevD.60.044004.

[196] J. Bicak, C. Hoenselaers, and B.G. Schmidt. The solutions of the einstein equations for uniformly accelerated particles without nodal singularities. ii. self-accelerating particles. *Proceedings of the Royal Society of London. A. Mathematical and Physical Sciences*, 390(1799):411–419, 1983. doi:10.1098/rspa.1983.0139.

[197] W. Kinnersley and M. Walker. Uniformly accelerating charged mass in general relativity. *Phys. Rev. D*, 2:1359–1370, 1970. doi:10.1103/PhysRevD.2.1359.

[198] E. Witten. Instability of the Kaluza-Klein Vacuum. *Nucl. Phys. B*, 195:481–492, 1982. doi:10.1016/0550-3213(82)90007-4.

[199] O. Aharony, M. Fabinger, G.T. Horowitz, and E. Silverstein. Clean time dependent string backgrounds from bubble baths. *JHEP*, 07:007, 2002. arXiv:hep-th/0204158, doi:10.1088/1126-6708/2002/07/007.

[200] R. Emparan and H.S. Reall. Generalized Weyl solutions. *Phys. Rev. D*, 65:084025, 2002. arXiv:hep-th/0110258, doi:10.1103/PhysRevD.65.084025.

[201] G.T. Horowitz and K. Maeda. Colliding Kaluza-Klein bubbles. *Class. Quant. Grav.*, 19:5543–5556, 2002. arXiv:hep-th/0207270, doi:10.1088/0264-9381/19/21/317.

[202] H. Elvang and G.T. Horowitz. When black holes meet Kaluza-Klein bubbles. *Phys. Rev. D*, 67:044015, 2003. arXiv:hep-th/0210303, doi:10.1103/PhysRevD.67.044015.

[203] H. Elvang, T. Harmark, and N.A. Obers. Sequences of bubbles and holes: New phases of Kaluza-Klein black holes. *JHEP*, 01:003, 2005. arXiv:hep-th/0407050, doi:10.1088/1126-6708/2005/01/003.

[204] S. Tomizawa, H. Iguchi, and T. Mishima. Rotating Black Holes on Kaluza-Klein Bubbles. *Phys. Rev. D*, 78:084001, 2008. arXiv:hep-th/0702207, doi:10.1103/PhysRevD.78.084001.

[205] H. Iguchi, T. Mishima, and S. Tomizawa. Boosted black holes on Kaluza-Klein bubbles. *Phys. Rev. D*, 76:124019, 2007. [Erratum: Phys.Rev.D 78, 109903 (2008)]. arXiv:0705.2520, doi:10.1103/PhysRevD.78.109903.

[206] D. Kastor, S. Ray, and J. Traschen. The Thermodynamics of Kaluza-Klein Black Hole/Bubble Chains. *Class. Quant. Grav.*, 25:125004, 2008. arXiv:0803.2019, doi:10.1088/0264-9381/25/12/125004.

[207] J. Kunz and S. Yazadjiev. Charged black holes on a Kaluza-Klein bubble. *Phys. Rev. D*, 79:024010, 2009. arXiv:0811.0730, doi:10.1103/PhysRevD.79.024010.

[208] S.S. Yazadjiev and P.G. Nedkova. Sequences of dipole black rings and Kaluza-Klein bubbles. *JHEP*, 01:048, 2010. arXiv:0910.0938, doi:10.1007/JHEP01(2010)048.

[209] P.G. Nedkova and S.S. Yazadjiev. Rotating black ring on Kaluza-Klein bubbles. *Phys. Rev. D*, 82:044010, 2010. arXiv:1005.5051, doi:10.1103/PhysRevD.82.044010.

[210] J. Kunz, P.G. Nedkova, and C. Stelea. Charged black holes on Kaluza-Klein bubbles. *Nucl. Phys. B*, 874:773–791, 2013. arXiv:1304.7020, doi:10.1016/j.nuclphysb.2013.06.013.

[211] M. Astorino, R. Emparan, and A. Viganò. Bubbles of nothing in binary black holes and black rings, and viceversa. *JHEP*, 07:007, 2022. arXiv:2204.09690, doi:10.1007/JHEP07(2022)007.

[212] L. Susskind. Computational Complexity and Black Hole Horizons. *Fortsch. Phys.*, 64:24–43, 2016. [Addendum: Fortsch.Phys. 64, 44–48 (2016)]. arXiv:1403.5695, doi:10.1002/prop.201500092.

[213] B. Kleihaus, J. Kunz, and E. Radu. d greater than or equal to five static black holes with S**2 x S**(d-4) event horizon topology. *Phys. Lett. B*, 678:301–307, 2009. arXiv:0904.2723, doi:10.1016/j.physletb.2009.06.039.

[214] B. Kleihaus, J. Kunz, E. Radu, and M.J. Rodriguez. New generalized nonspherical black hole solutions. *JHEP*, 02:058, 2011. arXiv:1010.2898, doi:10.1007/JHEP02(2011)058.

[215] R. Emparan. Black diholes. *Phys. Rev. D*, 61:104009, 2000. arXiv:hep-th/9906160, doi:10.1103/PhysRevD.61.104009.

[216] R. Emparan. Rotating circular strings, and infinite nonuniqueness of black rings. *JHEP*, 03:064, 2004. arXiv:hep-th/0402149, doi:10.1088/1126-6708/2004/03/064.

[217] R. Emparan and M. Gutperle. From p-branes to fluxbranes and back. *JHEP*, 12:023, 2001. arXiv:hep-th/0111177, doi:10.1088/1126-6708/2001/12/023.

[218] O.J.C. Dias, G.W. Gibbons, J.E. Santos, and B. Way. TBD. In preparation.

[219] H. Weyl. The theory of gravitation. *Annalen Phys.*, 54:117–145, 1917. doi:10.1007/s10714-011-1310-7.

[220] H.S. Tan and E. Teo. Multi - black hole solutions in five-dimensions. *Phys. Rev. D*, 68:044021, 2003. arXiv:hep-th/0306044, doi:10.1103/PhysRevD.68.044021.

[221] M. Astorino and A. Viganò. TBD. In preparation.

[222] R. Emparan, T. Harmark, V. Niarchos, and N.A. Obers. New Horizons for Black Holes and Branes. *JHEP*, 04:046, 2010. arXiv:0912.2352, doi:10.1007/JHEP04(2010)046.

[223] G.W. Gibbons, A.H. Mujtaba, and C.N. Pope. Ergoregions in Magnetised Black Hole Spacetimes. *Class. Quant. Grav.*, 30(12):125008, 2013. arXiv:1301.3927, doi:10.1088/0264-9381/30/12/125008.

[224] M. Astorino, R. Martelli, and A. Viganò. Black holes in a swirling universe. *Phys. Rev. D*, 106(6):064014, 2022. arXiv:2205.13548, doi:10.1103/PhysRevD.106.064014.

[225] B. Carter. Hamilton-Jacobi and Schrodinger separable solutions of Einstein's equations. *Commun. Math. Phys.*, 10(4):280–310, 1968. doi:10.1007/BF03399503.

[226] J.F. Plebañski. A class of solutions of Einstein-Maxwell equations. *Annals Phys.*, 90(1):196–255, 1975. doi:10.1016/0003-4916(75)90145-1.

[227] T. Levi-Civita. ds^2 einsteiniani in campi newtoniani. *IX. L'analogo del potenziale logaritmico, Rend. Acc. Lincei*, 28:101, 1919.

[228] W.B. Bonnor. Certain exact solutions of the equations of general relativity with an electrostatic field. *Proceedings of the Physical Society. Section A*, 66(2):145, 1953.

[229] K.S. Thorne. Absolute stability of melvin's magnetic universe. *Physical Review*, 139(1B):B244, 1965.

[230] E. Kasner. Geometrical theorems on einstein's cosmological equations. *American Journal of Mathematics*, 43(4):217–221, 1921.

[231] E. Poisson. *A Relativist's Toolkit: The Mathematics of Black-Hole Mechanics*. Cambridge University Press, 12 2009. doi:10.1017/CBO9780511606601.

[232] M. Alcubierre. The Warp drive: Hyperfast travel within general relativity. *Class. Quant. Grav.*, 11:L73–L77, 1994. arXiv:gr-qc/0009013, doi:10.1088/0264-9381/11/5/001.

[233] J. Lee and R.M. Wald. Local symmetries and constraints. *J. Math. Phys.*, 31:725–743, 1990. doi:10.1063/1.528801.

[234] G. Barnich. Boundary charges in gauge theories: Using Stokes theorem in the bulk. *Class. Quant. Grav.*, 20:3685–3698, 2003. arXiv:hep-th/0301039, doi:10.1088/0264-9381/20/16/310.

[235] G. Compère, K. Murata, and T. Nishioka. Central Charges in Extreme Black Hole/CFT Correspondence. *JHEP*, 05:077, 2009. arXiv:0902.1001, doi:10.1088/1126-6708/2009/05/077.

[236] M. Astorino. Removal of conical singularities from rotating C-metrics and dual CFT entropy, 7 2022. arXiv:2207.14305.

[237] M. Astorino. Embedding hairy black holes in a magnetic universe. *Phys. Rev. D*, 87(8):084029, 2013. arXiv:1301.6794, doi:10.1103/PhysRevD.87.084029.

[238] B. Linet. The static metrics with cylindrical symmetry describing a model of cosmic strings. *General Relativity and Gravitation*, 17(11):1109–1115, 1985. doi:https://doi.org/10.1007/BF00774211.

[239] J.A.G. Vickers. Generalized cosmic strings. *Class. Quant. Grav.*, 4:1–9, 1987. doi:10.1088/0264-9381/4/1/004.

[240] V.S. Manko and I.D. Novikov. Generalizations of the kerr and kerr-newman metrics possessing an arbitrary set of mass-multipole moments. *Classical and Quantum Gravity*, 9(11):2477–2487, nov 1992. doi:10.1088/0264-9381/9/11/013.

[241] D.M. Zipoy. Topology of some spheroidal metrics. *Journal of Mathematical Physics*, 7(6):1137–1143, 1966. arXiv:https://doi.org/10.1063/1.1705005, doi:10.1063/1.1705005.

[242] B.H. Voorhees. Static axially symmetric gravitational fields. *Phys. Rev. D*, 2:2119–2122, Nov 1970. URL: https://link.aps.org/doi/10.1103/PhysRevD.2.2119, doi:10.1103/PhysRevD.2.2119.

[243] R.M. Kerns and W.J. Wild. Generalized Zipoy-Voorhees metric. *Phys. Rev. D*, 26:3726–3727, 1982. doi:10.1103/PhysRevD.26.3726.

[244] C.M. Cosgrove. New family of exact stationary axisymmetric gravitational fields generalising the tomimatsu-sato solutions. *Journal of Physics A: Mathematical and General*, 10(9):1481–1524, sep 1977. doi:10.1088/0305-4470/10/9/010.

[245] C. Hoenselaers, W. Kinnersley, and B.C. Xanthopoulos. Symmetries of the stationary einstein–maxwell equations. vi. transformations which generate asymptotically flat spacetimes with arbitrary multipole moments. *Journal of Mathematical Physics*, 20(12):2530–2536, 1979. arXiv:https://doi.org/10.1063/1.524058, doi:10.1063/1.524058.